

Calcium-based models of synaptic plasticity

From fine-grain models to a light-weight rule for networks of spiking neurons

Author:

Simon LEBASTARD

Supervisor:

Dr. Jonathan TOBOUL

September 2018



école
normale
supérieure
paris-saclay



Contents

1	Introduction	2
1.1	Some elements on the anatomy and physiology of neurons	2
1.1.1	Composition and organization of neurons	2
1.1.2	Communication between neurons	3
1.2	Some elements on synapses and synaptic plasticity	5
1.2.1	Composition and physiology	5
1.2.2	Postsynaptic receptors as key components of synaptic transmission	8
1.3	Spike-Timing Dependent Plasticity	9
1.4	On simulating synapses	11
1.5	Calcium pathways and synaptic plasticity	11
1.5.1	The calcium hypothesis	11
1.5.2	Synaptic plasticity in neural networks	12
1.6	Content of the internship and modeling strategy	13
1.6.1	From phenomenological to detailed... and back!	13
2	Detailed modeling of calcium-calmodulin based synaptic plasticity	15
2.1	Identifying mechanisms for plasticity induction	16
2.2	Calmodulin-dependent protein kinase II and its role in synaptic plasticity	18
2.2.1	Calmodulin-dependent protein kinase II	18
2.2.2	Pathway leading to CaMKII activation	20
2.2.3	Action of CaMKII on synaptic strength	20
2.2.4	Modeling CaMKII activation	21
2.2.5	Modelling synaptic strength as a function of CaMKII activation	24
2.2.6	Simulation of the evolution of phosphorylation under minimal assumptions	27
3	From a detailed to a phenomenological model	31
3.1	Limitations of the base phenomenological model	34
3.2	Back to the detailed model: how can we bypass the Monte-Carlo trap?	35
3.3	Continuously stable phenomenological model	36
3.4	Analysis framework and results for the phenomenological model	38
3.4.1	Richness of the model	38
3.4.2	Experimental protocol	39
3.4.3	Defining STDP in our model	39
3.4.4	Fitting STDP behavior of hippocampal slices	39
3.4.5	Response of the model to Poisson firing	40
4	Network-wide properties of the calcium-based model	43
4.1	Network architecture and biological motivation	43
4.2	Implementation of calcium-based plasticity rule in the network	45
4.3	Future research directions	45
4.4	Conclusion	47
4.5	Our code	48
A	Appendices	53
A	Supplementary figures and tables	54

B Equations for the fine-grain model in the general case	56
B.1 Equations for the detailed model	56
B.1.1 Calmodulin binding to calcium	56
B.1.2 Calmodulin binding and phosphatase kinetics	57
B.1.3 CaMKII states	59
B.2 On solving the general CaMKII system	60
C Tentative models of action of CaMKII on synaptic strength	61
C.1 CaMKII binding to NMDA receptors	61
C.2 Phosphorylation of AMPA receptors	62
C.3 Quantification noise in the system	62
C.3.1 Noise on cytosolic variables	62
C.3.2 Noise at the membrane	63

List of Figures

1.1	Schematic representation of a neuron	3
1.2	Recording of membrane potential displaying different regimes of firing activity	4
1.3	Representation of an action potential propagating down an axon	4
1.4	Schematic representation of a chemical synapse	5
1.5	Long-term potentiation induced at a synapse from an hippocampal slice (in vitro)	7
1.6	Simplified representation of an AMPA receptor	8
1.7	A typical Hebbian STDP curve	9
2.1	Two potential mechanisms of synaptic plasticity that can account for spike-timing dependency	17
2.2	Mechanism proposed by Lisman for a bi-stable chemical switch	18
2.3	Representation of the second-messenger pathway stemming from post-synaptic calcium	19
2.4	Schematic representation of a CaMKII holoenzyme	22
2.5	Representation of chemical pathways in the model of Graupner and Brunel	22
2.6	Bifurcation diagram of active CaMKII as a function of postsynaptic calcium	23
2.7	Evolution of CaMKII activity in the model of Graupner and Brunel 2007	25
2.8	Transitions between the different states of CaMKII holoenzymes	26
2.9	Mechanism of AMPA receptor phosphorylation by CaMKII	27
2.10	Graph of the different CaMKII sub-unit states and their transitions	28
2.11	Example of behavior of our phenomenological model	29
3.1	Behavior of the phenomenological model of Graupner and Brunel 2012	32
3.2	Fitting of the phenomenological model of Graupner and Brunel 2012 to experimental data	33
3.3	Qualitatively different STDP curves are obtained from the phenomenological model of Graupner and Brunel	34
3.4	A trajectory of the system projected in the (calcium, activation level) plane	35
3.5	Response of recuperation variables and postsynaptic calcium concentration to spiking history	37
3.6	Fitting our model to experimental data from pyramidal cells in the hippocampus of mice	40
3.7	Dependency of STDP with frequency captured by our model fit	41
3.8	Response of our model to independent Poisson processes	42
4.1	Architecture of the network of Brunel 2000	44
4.2	regime of firing of neurons in the network as a function of outer excitation and inhibitory connections	44
4.3	Different global regimes of firing in the network of Brunel 2000	44
4.4	Spontaneous behavior of the network of 400 LIF neurons with our model of plasticity	46
B.1	Definition of the different reaction constants involving CaMKII	58
B.2	Different CaMKII sub-unit states and their transitions in the model of Michalski 2014	58

List of Tables

A.1	Value of synapse parameters used for the simulations presented in this report . . .	55
A.2	Value of network parameters used for simulation shown in Fig4.4	55

Abstract

Synaptic plasticity is widely believed to be responsible for learning and memory in neural populations (in particular in the mammal brain). The laws governing the strengthening and weakening of chemical synapses are only partly understood, for instance the nature of the information stored at a single synapse is itself very partly elucidated. Yet we know that some properties of synaptic plasticity, such as spike-time dependence, are of prime importance to explain the neural activity observed both in vitro and in vivo. In this regard, important efforts were undertaken in the last decades to develop models of synaptic plasticity, on a wide spectrum of complexity levels and resolution ranging from simplified phenomenological models to fine-grain models accounting for many chemical pathways and spatial compartments.

A specific type of models of plasticity, calcium-based models, focus on the concentration of postsynaptic calcium as the main proxy for synaptic plasticity. Some calcium-based models of plasticity exist, but they lack the computational simplicity to be implemented in networks of neurons. In an effort to understand the potential of such plasticity rules in learning time sequences and associations, we developed a light-weight plasticity rule that we successfully implemented in a network of several thousands neurons. Analysis of synaptic plasticity at the molecular level, especially through the study of protein CaMKII, was necessary to come up with this model. In this report, I explain our reasoning to develop the rule, study the behavior of a synapse who follows our model, as well as the behavior of a network of leaky integrate and fire neurons that are connected together with synapses that follow our model.

Acknowledgements

I would like to thank my advisor Dr. Jonathan Touboul for giving me the opportunity to work on synaptic plasticity at Brandeis. Through his supervision and interactions with the labs at the Volen Center and beyond, I was able to explore both biology and computational neuroscience, in a challenging but fascinating quest to better understand the basic units of memory in our brain. His ideas and feedback were often crucial, both on technical subjects and on working in academia. Most importantly I enjoyed working with him and sharing ideas.

I would also like to thank Dr. Laurent Venance at Collège de France for providing us with experimental data, and equally importantly feedback on the questions that I had in electrophysiology. Interactions with the lab at INSERM allowed me that have both inputs from the computational side and from the experimental side, which I think turned out very valuable.

Sincere thanks to Dr. Paul Miller for welcoming me in his lab, and giving me the opportunity to share my work with teams of experimental neuroscientists.

Finally, thanks to Charlotte Piette, Denis Patterson, Yi Cui, Ben Ballintyn, Bolun Chen for the good moments at Brandeis!

Chapter 1

Introduction

This project revolved around modeling events that occur at synapses, the interface between neurons. Those events are intrinsically of physical and chemical nature; an introduction to the basic physiology of neurons and synapses is therefore appropriate to make sense of the models that will be introduced further. Here I will provide a brief introduction to neurons and synapses, from which I can provide the motivation for this project. I will then introduce the current state of knowledge on synaptic plasticity, with an emphasis on the current modeling efforts.

1.1 Some elements on the anatomy and physiology of neurons

Neurons (also called nerve cells) are the main type of cells found in the nervous system (both peripheral and - what we usually refer to as the brain - central nervous system). They are considered the base unit of communication and processing of information. Neurons play a critical role in processing important information both locally (a simple case in point is the mono-synaptic reflex system that can be found for instance at the knee jerk) and through the CNS.

There are some other types of cells, such as glia, that are significant in number, and whose function and interactions with neurons are increasingly grasped as important. However, these cell types do not play a significant part as a "first order approximation", and I will choose to overlook their existence and effects.

1.1.1 Composition and organization of neurons

Throughout this section I will use the terms "downstream" and "downward" to refer to the transfer of information from a neuron to another. This information communication is most often unidirectional; it thus makes sense to refer to a "downward" direction and to the neurons "downstream" of a given neuron. However, if neuron B is downstream of neuron A, it is very much possible for neuron A to be downstream of neuron B as well, as B can connect "back" to A, so that A and B have reciprocal connections. In this report I will use the notation $A \rightsquigarrow B$ when A and B are neurons, as the statement "neuron A is upstream of neuron B", which does not in itself imply that there is a synapse from A to B. I will also use the notation $A \rightarrow B$ either to indicate that B is directly downstream of A (ie $A \rightsquigarrow B$ and there is a synapse from A to B), or to refer to the synaptic connection from presynaptic neuron A to postsynaptic neuron B (see 1.1.2 for definition of those terms). Finally, when more than one chemical synapse from A to B exists, I will use notation $A \Rightarrow B$ to refer to all synapses from A to B, instead of just on chosen arbitrarily.

Neurons can be described with the following components:

- their nucleus in the **soma**. This is where the genetic information is stored
- a single **axon**, that is used to generate electrical signals that are transmitted to downstream neurons

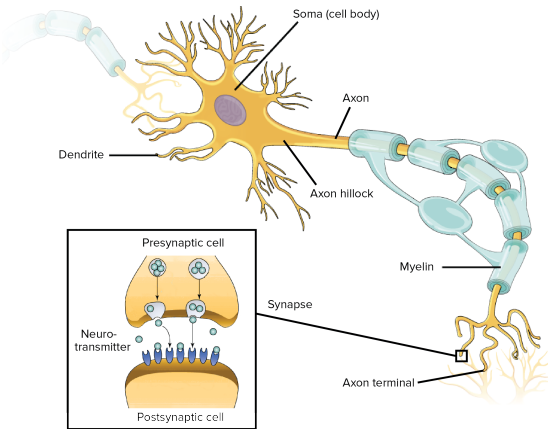


Figure 1.1: Schematic representation of a neuron. Electrical information is transmitted from upstream neurons via the connection that they make to the dendrites, at so-called synapses. Such electrical potential passively propagates within the neuron. The depolarization effect from multiple upstream neurons can accumulate past the soma where the nucleus, that comprises the genetic information of the cell, is stored. A depolarization of the axon above a critical quantity leads to the emission of a sharp depolarization, termed action potential, that propagates down the axon. This action potential is to be translated to chemical information at synapses

- the axon splits into multiple synaptic branches that target different downstream neurons. Each synaptic branch terminates at one or more **synapses**. A synapse is the connection point between a **presynaptic neuron** ('upstream'), and a **postsynaptic neuron** ('downstream').
- **Dendrites** are the postsynaptic branches that allow the electrical information transmitted by upstream neurons to flow down to the neuron axon.

1.1.2 Communication between neurons

Given those non-extensive elements of presentation, it is now essential to point out that communication between neurons is mostly of discrete nature. Neurons communicate via **action potentials** (or spike), that are spikes of electrical potential that travel down the axon, all the way to the presynaptic terminals. The membrane of the whole neuron is polarized at rest state (roughly -70mV for human neurons, as measured with mass in the extra-synaptic medium). Ion channels on the axon membrane allows for changes in membrane potential. When depolarized past a given threshold voltage, an action potential (ie, a spike of voltage) is generated and propagates down the axon (causing the threshold to in turn be crossed further down the axon). Depending on the upstream activity, a neuron can fire a single action potential, or a sequence of action potential, for instance at a fixed rate. Such sequences are generally called **spike trains** of action potentials. In what follows, I will need to refer to examples of AP and spike trains. I will denote t_A the time of an action potential fired by neuron A , and $(t_A^{(i)})_{i \in I}$ a spike train from neuron A , as a sequence of spikes, ordered in increasing emission times.

There have been much debate as to whether the information that is effectively treated from one neuron to another is encoded in the exact spike timing or rather in statistics such as the spike rate. The current consensus is that both fine-grain timing and rate come into play in encoding, with relative importance depending on the regime of firing itself (when the neuron fires sparsely, exact timing is more likely to carry information).

Note that sub-threshold dynamics are also deemed to be important. When we look at network of neurons in the last chapter of this report, we will come back to sub-threshold dynamics. Until then, I will ignore this aspect and focus on spiking activity.

In turn, an action potential reaches presynaptic terminals and allows for the transmission of information to the postsynaptic neuron through the synapse.

Even though the signal does propagate by electrical means down the axon, the information is not necessarily transferred to downstream neurons this way. Synapses can be of two types:

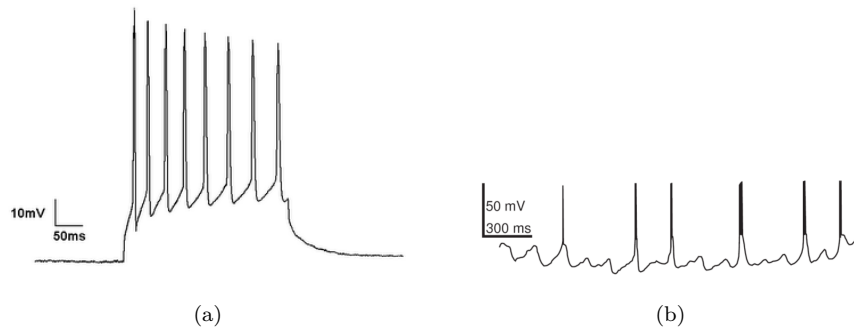


Figure 1.2: Recording of membrane potential displaying different regimes of firing activity. **A:** A Spike train of frequency $\backslash 20\text{Hz}$. **B:** A spike train with some sub-threshold oscillations taking place

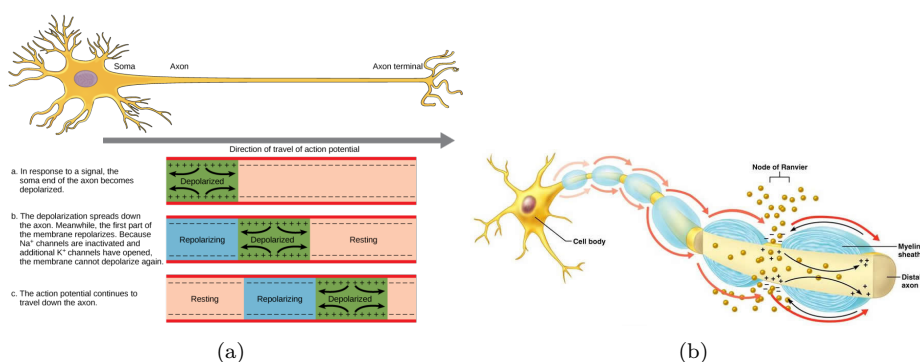


Figure 1.3: The most important part of the electrical information carried on by a neuron is of discrete nature, and is called an action potential. A wave of depolarization of the axon membrane propagates down the axon, followed by a wave of re-polarization. Generation and propagation of the **action potential**(AP) is allowed by the presence of many ion channels at the surface of the membrane, that can let ions in and out of the membrane and locally alter its potential. For more information on the generation and propagation of AP, see **Kandel**

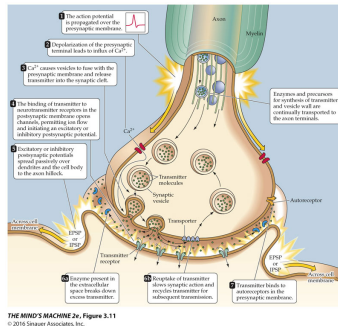


Figure 1.4: Schematic representation of a chemical synapse. Courtesy of Watson & Breedlove, **MindsMachine**

- Electrical synapses can allow for the rapid flow of information. There is almost no delay in the transfer of information with the synapse, which make of electrical synapses tools fit for the transmission of simple information, priority information. However, such synapses offer very limited plasticity, and are therefore not deemed to account for information storage in the brain.
- **Chemical synapses** are much more sophisticated, as well as much more important for information storage within the brain and nervous system. Even though more time is necessary to transmit a signal from the presynaptic to the postsynaptic neuron, the chemical synapse is a very complex system that allows for flexibility in the processing and storage of information based on past history of stimulation. The much richer repertoire of chemical synapses explain why they are more of interest in our case.

By referring to synaptic plasticity in this report, I will always mean synaptic plasticity at chemical synapses. I will now overlook electrical synapses altogether and focus solely on chemical synapses.

1.2 Some elements on synapses and synaptic plasticity

1.2.1 Composition and physiology

There is a variety of synapses in the human brain, with important dependence on location (cholinergic synapses at the interface with muscles are different - somewhat simpler - from synapses in the forebrain) and on the neurotransmitter that is released (see further).

Fig.1.4 depicts the different steps of signal transmission at a chemical synapse. The membrane at the presynaptic button contains **calcium-specific ion channels** that open in response to depolarization. The influx of calcium ions into the presynaptic button causes the release of **synaptic vesicles** into the synaptic cleft (see next §). Those synaptic vesicles are stores of neurotransmitters that accumulate on the presynaptic side and respond to calcium influx. Each of these vesicles contain several thousands molecules of **neurotransmitters**. The exact nature of the neurotransmitter that is released depends on the neuron (acetylcholine at the neuromuscular junction, glutamate for many neurons in the brain)

Such an influx of calcium occurs upon arrival of an action potential at the presynaptic button, coming from the axon of the presynaptic neuron. With some intrinsic variability due in part to synaptic plasticity, a vesicle is then expelled from the presynaptic button into the **synaptic cleft**, which is the region at the interface between the **presynaptic button** and the **postsynaptic button**. The neurotransmitters then diffuse within the cleft and bind to receptors specific to them on the postsynaptic side. Upon binding of neurotransmitters, those receptors open and let ions flow into the postsynaptic button. This causes a local change in the membrane voltage that can propagate to the axon of the postsynaptic neuron. Please note that for the depolarization of a single dendrite is generally not enough to cause the postsynaptic neuron to fire an action

potential. Instead, depolarization from multiple dendrites cumulate their effect at the soma and can, together, cause an action potential. This phenomenon is referred to as **cooperativity**.

Neurons can be either **excitatory** or **inhibitory**, with different neurotransmitters and synapse composition depending on that. An action potential arriving at the presynaptic side of an excitatory synapse (generally a synapse releasing glutamate) will cause a **local depolarization** on the postsynaptic side, while an inhibitory synapse (generally releasing GABA or glycine) will cause a **local hyperpolarization**.

The chemical synapse is a complex object. It comprises a network of hundreds of chemical compounds which regulate their respective activity and affect synaptic properties, both on the presynaptic and postsynaptic sides. It is currently believed that synaptic plasticity is carried on by multiple mechanisms, that leverage both chemical (phosphorylation of kinase proteins, for instance) and structural changes (growth of the synapse, modification in cytoskeleton structure...). Chemical and structural modification of the synapse will generally involve a modification of the size of the postsynaptic depolarization evoked by a given presynaptic signal. We then say that the strength of the synapse is modified. We therefore define the **synaptic strength** ρ as the ratio between the postsynaptic response and presynaptic input:

$$\rho = \frac{\mu(\Delta V_{post})}{\mu(\Delta V_{pre})}$$

where μ measures either the presynaptic and postsynaptic depolarization or the presynaptic and postsynaptic currents, respectively ΔV_{pre} and ΔV_{post} .

Say we are studying a synapse whose presynaptic neuron is excitatory. When looking at voltages, the change in polarity that results at the postsynaptic spine is called a **Excitatory Post Synaptic Potential (EPSP)**. When looking at currents, the change in intensity is called a **Excitatory Post Synaptic Current (EPSC)**. Note that there are different ways of measuring such a depolarization at the postsynaptic side since the output signal is not necessarily discrete. We can either measure the maximum amplitude of depolarization, or its integral. In what follows we choose to refer to the maximum amplitude of the resulting voltage or current.

The fact that synaptic strength can be modulated is called **synaptic plasticity**. A synapse that, following an event, sees its synaptic strength increased is said to be **potentiated**. On the other hand, a synapse that sees its synaptic strength decreased is said to be **depressed**.

Some landmarks experiments on hippocampal neurons (Bi and Poo 1998) found that depending on how the voltages of both on the presynaptic and postsynaptic sides are controlled, the synapse will potentiate or depress (see 1.5 for an example of long-term potentiation) This experiment is tightly linked to the concept of STDP, which is introduced further down.

Changes in synaptic strength can occur on several time scales. Changes on the order of milliseconds to a second are called **Short-Term Plasticity**. This type of plasticity accounts for the fact that synaptic strength in response to a train of action potentials, such that the synapse will respond more intensely to the first few spikes than to the next spikes. On the other hand, some changes can last from seconds to years. Mechanisms for such changes are deemed to be responsible for learning and memory in general. We then speak of **Long-Term Plasticity**. When the synapse is potentiated (depressed), it is common to speak of **Long-Term Potentiation(LTP)** and **Long-Term Depression(LTD)**, respectively.

LTP itself comprises multiple types of mechanisms. It is believed that while mostly chemical processes are involved in storage the information in the first tens of minutes after stimulation at the synapse, this information could then be translated to epigenetic and structural changes for it to last from hours to years. We thus differentiate between an **early LTP** (or e-LTP, only chemical) and a **late LTP** (or l-LTP chemical, structural and epigenetic).

Those distinctions are important for the computational neuroscientists who aim at modeling synaptic plasticity: should they focus on presynaptic, postsynaptic mechanisms, or both? Do they want to look at Short-Term plasticity, e-LTP, l-LTP? This would all depend on what they are trying to demonstrate in the first place.

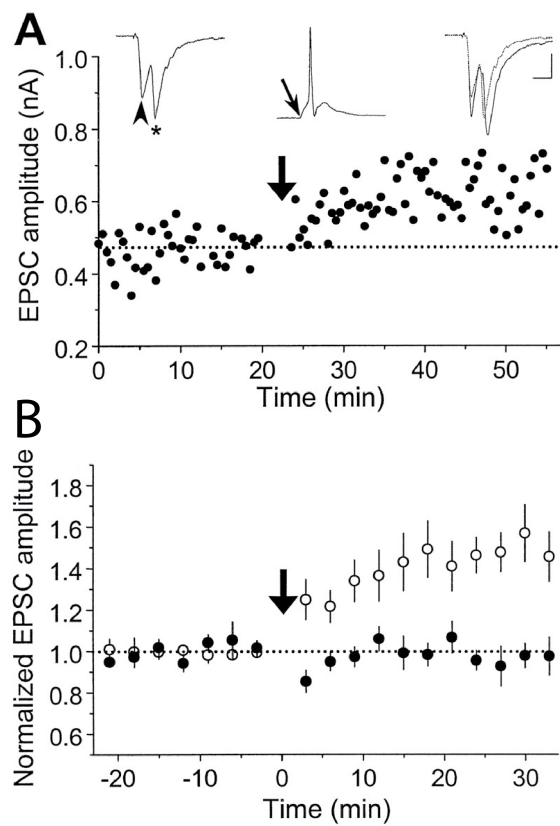


Figure 1.5: Long-term potentiation induced at a synapse from an hippocampal slice (in vitro). The postsynaptic voltage is clamped at a high value, and 60 pulses of presynaptic voltage at frequency 1Hz are induced. **A:** EPSC as a function of time for a single trial, with the induction protocol described. **B:** Average results of the evolution of EPSC in the absence (white dots, $n = 14$ trials) or in the presence (black dots, $n' = 5$ trials) of d-AP-5, an inhibitor of plasticity

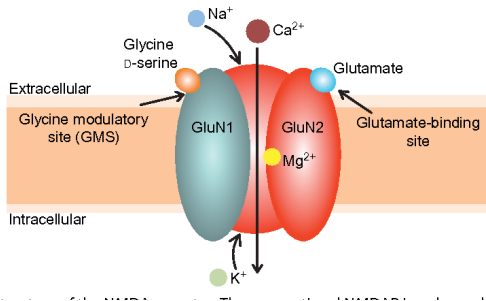


Figure 1.6: Simplified representation of an AMPA receptor. At rest membrane potential, a magnesium ion blocks the channel, so that even when bound to glutamate, the channel won't open. When the postsynaptic membrane is depolarized, the magnesium ions unbind from the receptor, transiently allowing its activation. Simultaneous presence of glutamate and depolarization of the postsynaptic membrane are therefore necessary for the opening of the receptor

1.2.2 Postsynaptic receptors as key components of synaptic transmission

As previously stated, stimulation on the presynaptic side causes the release of vesicles of neurotransmitters in the synaptic cleft, that in term activate ion channels on the postsynaptic side. These ion channels (or receptors) are of different kinds. Here I need to introduce three of them, as they play a key role in the models that were investigated. All three receptors are called **ionotropic receptors** since they act upon the postsynaptic button by controlling the amount of ions that can flow within it. Another important characteristic of such channels is that they are only permeable to ions when activated by a specific neurotransmitter, coming from the synaptic cleft. Some receptors, for instance, are activated by acetylcholine, others are activated by glutamate...

AMPA receptors (or AMPAr) are ion channels that are permeable mostly to K^+ and Na^+ ions. Such channels can open and let those ions flow into the presynaptic button, resulting in its depolarization. Those channels are also modulated by a specific neurotransmitter, amino-acid glutamate. The receptor will only open when one or multiple molecules of glutamate from the cleft binds to it. It can then allow ions in or out, until it closes by deactivation, due to the neurotransmitter unbinding from it, or from the action other external regulators. Figure 1.6 provides a schematic representation of an AMPAr.

Another type of ionotropic receptor is the **Voltage-Dependent Calcium Channel** (VDCC). This type of receptor works similarly to the AMPA receptor, but is mostly permeable to Ca^{2+} ions. When activated by their neurotransmitter, they become permeable to calcium ions, allowing for fast depolarization of the postsynaptic membrane.

I will finally mention **N-methyl-D-aspartate** (NMDA) receptors, which play a critical role especially in calcium-based models of plasticity. Modulated by glutamate, they are somewhat more complex than AMPA receptors, in that binding of glutamate on the extra-synaptic side is not sufficient for activation. Because of passive blocking of the channel by magnesium at rest membrane potential, it is also necessary that the postsynaptic membrane be already depolarized for the NMDA receptor to open. In this way, NMDA receptors play a role of **coincidence detector** of spiking activity of the presynaptic neuron (via activation by neurotransmitters from the presynaptic side), and spiking from the postsynaptic neuron (via the depolarization of the postsynaptic membrane that result from back action potentials). As a result, NMDA receptors play a key role in spike-timing dependent plasticity.

Activated NMDA receptors are permeable mostly to Ca^{2+} ions. Their activation is often slower than that of VDCC channels, but with longer lasting effects.

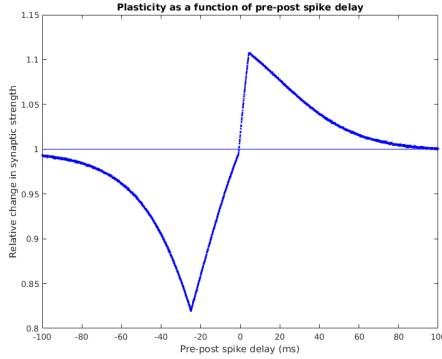


Figure 1.7: A typical Hebbian STDP curve. The x-axis represents the delay between the presynaptic spike and the postsynaptic back Action Potential. A positive delay indicates that the presynaptic spike occurred before the postsynaptic spike. The y-axis indicates the relative change in synaptic strength. The plasticity is indeed Hebbian in this case, as a "causal" turn of events leads the synapse to potentiate

1.3 Spike-Timing Dependent Plasticity

A great deal of effort was undertaken in the last 20 years to understand and classify the rules that govern synaptic plasticity. A fundamental aspect of this plasticity is that it is "loosely supervised". Let's take the example of a synapse $A \rightarrow B$. The signal for supervision can be understood as "did neuron A make neuron B fire, and if so, when?". For a rule of plasticity to incorporate this information, there must be some feedback of information, for the synapse to "know" that the (downhill) soma of neuron B fired an action potential. This phenomenon naturally occurs when B fires: the spike that is generated at its axon, close to the soma, can also passively propagate up the dendrites; it can travel "upwards", in other words. After all, dendrites are neither electrically isolated from the soma, nor do they intrinsically allow only for unidirectional conduction. The action potential traveling "upwards" is called a **back Action Potential** (bAP). It can travel up to all synapses in its path, and carries the signal that is believed to be used for supervision.

To summarize the last point, a synapse can adapt its functioning based on the relative timing of action potentials fired both at the presynaptic and at the postsynaptic neurons. This phenomenon was called **Spike-Timing Dependent Plasticity (STDP)** (see Song Sen 2000), and is one of the core concepts of this project. A landmark study of the phenomenon was led by Bi & Poo in 1998 (Bi and Poo 1998), where they emit hypothesis on both the nature of STDP (additive for positive time delays, multiplicative for negative time delays) and the shape of it (a change that depends exponentially on the delay, with two separate rules for positive and negative delays). For recent reviews of the history and state-of-the-art knowledge on STDP, see DE 2012 and Markram, Gerstner, and Sjöström 2012.

Throughout the report I will need to refer to examples of spike timing. With $A \rightarrow B$, I will denote $\delta t = t_B - t_A$ when only a single presynaptic and a single postsynaptic spikes are involved. Even though many spikes are generally involved on both sides, focusing on a single pair can be conceptually useful.

A natural question to ask about STDP is the following: in our last example, synapse $A \rightarrow B$ is indeed able to know that an action potential was fired by B, but how is it supposed to know that it contributed to B firing in the first place? What if a synapse $A' \rightarrow B$ caused B to fire, and synapse $A \rightarrow B$ simply receives a resulting bAP, without having any causality link to the action potential? The answer lies in the fact that chemical synapses have ways to "tag" their own activity for various periods of time. Activation of the synapse results in tagging. If shortly after this event a bAP is received at the synapse from the postsynaptic side, the tag is there to indicate that the synapse contributed to the postsynaptic firing event.

STDP is of uttermost theoretical importance because it allows to get information on causality for learning. This information can act as a basic building bloc for powerful behaviors at the level

of neural networks. It is believed that as early as 1890 William James foresaw the interest of spike-timing for learning habits. It was more accurately framed by Donald Hebb (Hebb 1988). A Hebbian learning rule is a rule that enforces two criteria:

- in which neurons (connected together by a synapse) that fire in causal order will tend to reinforce their synaptic connection. In our previous example, the synapse between A and B would be Hebbian if a close succession of events "A fires" and "B fires" reinforces the synapse between the two.
- neurons that fire in an anti-causal manner reduce their synaptic connection. So if the two events "B fires" then "A fires" follow closely, the synapse between the two would weaken.

The theory is often summarized as "**Cells that fire together, wire together. Cells that fire out of sync, loose their link**".

Hebbian learning is known to be implemented in the neocortex and in the pyramidal neurons of the hippocampus. But without having this fact in hand, one can already see that such a rule is powerful for shaping neural networks so as to predict outcomes of events. For instance, two populations of neurons coding for visual sensory inputs can learn to encode for the fact that a visual input ("the door handle twists") often empirically lead to another visual output ("the door opens"). Thus the prediction that the two events are causally connected can be learned. In this way a prediction that the door will open will be made way before the door actually opens. Such a scheme is very generic, and one needs to realize that being able to make accurate prediction bears a large survival value.

In a similar manner, Hebbian learning allows for learning of temporal patterns or correlations. For instance, in songbirds such as the zebra finch, neuron nuclei responsible for generating patterns of notes are deemed to be governed by such rules, and temporal patterns of note generation are learned by listening to peer songbirds (see Hahnloser, Kozhevnikov, and Fee 2002). Another application of Hebbian learning is the spontaneous generation of spike patterns that can be useful for motor functions.

Note that Hebbian learning presents the other advantage of being able to mitigate the impact of feedback on synaptic plasticity, with a stabilizing effect. Imagine in our example that neuron B connects back to neuron A...

Anti-Hebbian theoretical properties are less understood, but some authors suggest that the phenomenon could allow for computation of differences, with an interesting consequence in the fact that known pattern could be "subtracted" from the prediction produced by the network, so that other novel components could be better represented. Moreover, by keeping distal synapses weak, this LTD could enforce greater synchrony in firing and create a fundamental different in the role of proximal and distal synapses.

The laws governing the behavior of a synapse are complex, and multiple factors join or restrict spike-time dependency. Consider for instance the dependence on spike train frequency. In most areas where Hebbian learning is seen, only Long-Term Depression is seen at low frequencies, regardless of spike timing. At large frequencies, only Long-Term Potentiation is observed. There is thus a range of frequencies in which proper STDP is observed. Moreover, one must keep in mind the stochastic nature of action potentials, due in part to the many sources of noise (quantification noise from ion channels or chemical compounds in limited supplies or constrained in space, for instance). In this way, spiking events are generally regarded as point processes with random spike times. Of course, those random events are to a large extent influenced by the activity of upstream neurons (as well as regulatory processes, internal like epigenetic or external like glial). Moreover, one must note that there is no reason why the information relevant to plasticity would be captured by pairs of spikes. Pfister and Gerstner 2006 showed that triplets of successive spike events captures much more information on synaptic plasticity. In general, it is believed that the whole history of both presynaptic and postsynaptic spikes come into play through biological quantities that drive plasticity. Among one of the leading hypothesis is the fact that the quantity of postsynaptic calcium controls plasticity through multiple chemical pathways.

In this regard, one must consider STDP less like a fundamental mechanism of plasticity than like a property of synapses that capture some part of their learning rules in link with causality, or the absence of it.

After this word of warning on the place of STDP in learning, we can mention that there is experimental data providing insights on the way causality would be computed at the synapse. Considering our example $A \rightarrow B$, Bi and Poo 1998 found that for dissociated rat hippocampal neurons, positive delays between $\delta t = t_B - t_A$, changes in synaptic strength are proportional to the initial value of synaptic strength w_0 ($\Delta w \propto w_0$ in a multiplicative fashion), while for negative δt , the change in synaptic strength is mostly independent on w_0 , ie the update in synaptic strength is additive.

Additive and multiplicative learning rules have been designed and studied by multiple authors (see Gerstner et al. 1996). Even though such rules are purely phenomenological and fail to capture the role of any biological lever on plasticity, they provide computationally simple rules. If such rule can faithfully reproduce the behavior of synapses, they would then have the virtue of simplicity, which is important when investigating the influence of plasticity in a large network of neurons. Another approach has been favored in our work, in line with pioneering models like Shouval, Bear, and Cooper 2002 and Abarbanel2003. The approach is to simulate the evolution of the biological quantity relevant to plasticity through a simple rule, and have the synaptic weight depend on this quantity through time. Such rules can achieve, at a similar level of complexity, a greater level of accountability regarding biological phenomena and transparency as per the meaning of their parameters.

1.4 On simulating synapses

One of the challenges of neuroscience is to explain experimental data from basic chemistry and physics. In particular, an important corpus of literature focuses on building models of synaptic plasticity that can account for spike-timing dependency, and the influence of frequency and number of stimulations on the plasticity, among others. However, the very large number of chemical species and the intricate dynamics of their interaction and action on the synapse make straightforward modeling very challenging. Some softwares (**NeuronSoft**) have emerged to model neural and synaptic dynamics in fine detail, based on the chemical dynamics of up to hundreds of chemical species, with the possibility to have spatial and/or partitioned models. If such models can be developed, they are mostly used to help understand how the complex network of chemical species give rise to some properties of the neuron or of the synapse. They are used to simulate a single synapse, or maybe a few when large populations of synapses, in particular they cannot be used to study a network of neurons.

To simulate a system containing a large number of synapses (from thousands to millions or more), only simple, light-weight models can be used. Since it is believed that much of the mechanisms relevant to learning occur at the network level, such high-level modeling is important. However those models must capture the important properties of the synapse. This simplification task is left to computational neuroscientists, who can take one of several approaches:

1. **Top-down approach:** synthesize state-of-the-art research in electrophysiology to focus on a few coarse-grain biological processes, simplify their dynamics into a low-dimensional model
2. **Flat approach:** build a purely phenomenological model, by fitting to available experimental data a low-dimensional model

1.5 Calcium pathways and synaptic plasticity

1.5.1 The calcium hypothesis

We have seen that some synaptic receptors are permeable to calcium ions (VDCC and NMDA receptors). Works by Malenka and Lisman among others (see Malenka et al. 1988, John Lisman 2017, Rossetti et al. 2017) have shown that calcium influx into the postsynaptic cell is both necessary and sufficient for the induction of both LTP and LTD through the action of increasingly well-known proteins. The calcium hypothesis stipulates that chemical pathways stemming from post-synaptic calcium are responsible for the induction of synaptic plasticity.

Works by Lisman et al (Lisman 1989, John Lisman, Schulman, and Cline 2002, Faas et al. 2011, Sanhueza and John Lisman 2013) have shed light on the mechanisms of potentiation and depression of synaptic strength, although a comprehensive view of the whole pipeline is still missing. The

first section of this report looks at some detailed models of calcium-based synaptic plasticity, and expand on those mechanisms.

This partial understanding of the chemical pathway to plasticity has allowed computational neuroscientists (Shouval, Bear, and Cooper 2002 and Abarbanel2003) to come up with first calcium-based, phenomenological models of synaptic plasticity. Those models were completed and perfected by authors like Graupner and Brunel (Graupner and Brunel 2012, the model we started from in our analysis), who could also benefit from more recent advances in the understanding of plasticity at the molecular level. From the study of detailed models of calcium-induced plasticity, they were able to come up with phenomenological models that take a history of calcium concentration as the key variable to synaptic plasticity. The second chapter of this report focuses on such a model, and explains its shortcomings as far as implementing a network of neurons with plastic synapses is desired.

To get a fairly recent overview of biophysical models of synaptic plasticity (with an emphasis on the calcium hypothesis), see Graupner and Brunel 2010.

1.5.2 Synaptic plasticity in neural networks

In the last two decades, networks of spiking neurons have been widely investigated for many models of neurons (LIF, Izhikevich, theta...) and many network architectures. However, most of the literature focuses on properties of such networks, the influence of the model of neuron or of the statistics of some input signal. The behavior of a network of spiking neurons with plastic synapses has received less attention. One of the main reasons why is that simulating a network of neurons with plastic synapses is computationally very demanding. A fully-connected network of 10000 neurons would represent 10^8 synapses. As a remainder, an adult human brain contains about 10^{11} neurons, with a single neurons making on average 10000 connections with other neurons in the human brain.

Therefore, the only case when such a network can be simulated is when the behavior of each synapse is governed by computationally simple rules.

Some studies looked at the behavior of networks of spiking neurons where synapses follow STDP rules that only look at pairs of spikes. In particular, additive rules of STDP (rules that can be formulated as $\Delta w = f(dt)$ in contrast to multiplicative rules, which look like $\frac{\Delta w}{w} = f(dt)$) that look at pairs of spikes are easy to use. Ocker, Litwin-Kumar, and Doiron 2015 developed a theory of how a network of LIF neurons behaves when the synapses follow the classic additive rule from Gerstner et al. 1996:

$$\Delta w = \begin{cases} \Theta(w^{max} - w)f_+ \exp\left(-\frac{|s|}{\tau_+}\right) & \text{if } s \geq 0 \\ \Theta(w)(-f_- \exp\left(-\frac{|s|}{\tau_-}\right)) & \text{if } s < 0 \end{cases}$$

where $\Theta(\cdot)$ is the Heaviside function f_+, f_-, τ_+, τ_- are positive parameters.

The theory, although powerful enough to predict the evolution of some statistics of the network (fixed points for average weight and other first momenta for the synaptic weights), does not extend in the case of multiplicative STDP rules, which are increasingly believed to better represent the behavior of the synapse, especially for positive time delays. Moreover, STDP rules such as Gerstner et al. 1996 are limited to spike pairs, and base use as the base element for plasticity the time delay between PRE and POST spikes. Looking at pairs of spikes has proved limited in terms of how much of the experimental data can be reproduced. One assumption formulated by Pfister (Pfister and Gerstner 2006) is that consecutive spike triplets (for instance POST → PRE → POST), instead of spike pairs (for instance PRE → POST), could be a good predictor of the plasticity behavior. Another approach is to have plasticity models that instead use a biological trace of plasticity such as postsynaptic calcium concentration.

Our work pushes further the effort to have a calcium-based model of synaptic plasticity as a light-weight rule that can be implemented in a neural network. From there, we could investigate the behavior of a network where synapses are ruled by our model, and study the properties that this type of plasticity provides the model. As one of the main questions that one could then answer would be: can we actually learn time sequences such as songs or movies to a network using this sort of plasticity?

1.6 Content of the internship and modeling strategy

Here is a summary of what our efforts have been targeted to during the internship.

Main questions

- Laurent Venance (INSERM) provides us with data mice on synaptic plasticity in response to given protocols of excitation of pre and post neurons. *How do synapses encode information? Is this information digital, like Malenka et al. 1988 and O'Connor, Wittenberg, and S. S.-H. Wang 2005 suggest? Can the data provided by the Venance lab fit the assumption of bi-stable synapses?*
- As explained further in this report, the calcium-based plasticity rules that we know of are too computationally costly to be readily implemented in a network of spiking neurons. *How can we develop a plasticity rule that is light enough to be implemented in a network of at least 1000 neurons, so that we can start to investigate calcium-based plasticity for its effects in networks?*

Goals We had two main goals:

- *Develop a model of synaptic plasticity that is computationally simple*, so that we can later investigate a network of spiking neurons that have synapses that can evolve with time. With an actionable rule of synaptic plasticity, one can try to train a network to perform some tasks, for instance to remember a specific signal, in a sense that we will define later. In particular, as synapses that present STDP are believed to contribute to learning of time sequences at the network level, we aim to use a network of plastic neurons to learn time-dependent signals such as songs or sequences of movies
- *Investigate the nature of the synaptic code* by comparing the performance of models of bi-stable synapses with models of continuously stable synapses, and their capacity to fit the experimental data from the Venance lab.

1.6.1 From phenomenological to detailed... and back!

Our initial approach to solve those questions has been to look at phenomenological models of plasticity that can explain experimental data but fail to easily port to networks, and try to come up with our own.

One of the models that inspired the project was the calcium-based phenomenological model by Graupner and Brunel (Graupner and Brunel 2012). The model looked at a single synapse between a presynaptic neuron A and a postsynaptic neuron B. It linked the spike history of neuron A and that of neuron B to influxes of calcium ions into the postsynaptic density. The plasticity behavior of the synapse is then a direct function of the calcium concentration, according to two thresholds that the calcium must top respectively to depress and potentiate the synapse. Plasticity of the synapse is thus governed by a stochastic equation that depends on the value of calcium concentration.

This model combines computational simplicity with a great flexibility. It is simple enough so that solutions can be derived analytically in some cases of initial conditions, yet it can mimic the behavior of many synapses with qualitatively different plasticity behaviors (see Fig2 from Graupner and Brunel 2012), and offers great interpretability of the parameters involved. In this regard, different sets of parameters can reflect different conditions corresponding to synapses of different types of neurons, or differences in distance of the synapse from the soma ("proximal" synapses are often deemed to be potentiated more easily than "distal" synapses).

Let $(t_A^{(i)})_{i \in I}$ be the sequence of sorted spike times coming from synapse A, and $(t_B^{(j)})_{j \in J}$ be the sequence of sorted spikes times for B. In the model, the postsynaptic calcium concentration follows the following equation:

$$\tau_c \frac{dc}{dt} = -c(t) + C_{pre} \sum_{i \in I} \delta(t - t_A^{(i)} - D) + C_{post} \sum_{j \in J} \delta(t - t_B^{(j)})$$

so that a postsynaptic spike would instantly confer a bump C_{post} to the calcium concentration, and a presynaptic spike would confer a bump C_{pre} after a delay D . This delay can account for

the higher transmission time due to propagation of the signal through the cleft, as well as the difference in time propagation from soma to synapse.

A scaled synaptic strength variable $\rho \in [0, 1]$ then undergoes variation according to the following equation:

$$\tau_\rho \frac{d\rho}{dt} = f(\rho) + \gamma_p(1 - \rho)\Theta(c(t) - \theta_p) - \gamma_d\rho\Theta(c(t) - \theta_d) + \zeta(t)$$

where $\zeta(t)$ is a Gaussian noise given by:

$$\zeta(t) = \sigma \sqrt{\tau_\rho} \sqrt{\Theta(c(t) - \theta_p) + \Theta(c(t) - \theta_d)} \eta(t)$$

The thresholds are generally taken such that $\theta_d < \theta_p$. There is a good reason why that would be the case, that will become evident when we look at molecular models of plasticity. Here $\Theta(\cdot)$ is the Heaviside function. Also note that the noise itself is function of these Heaviside, so that the stochastic component only manifests when the calcium level exceeds at least one threshold.

Therefore, for calcium concentrations below both thresholds ($c(t) < \theta_d < \theta_p$), the dynamic solely depends on the term $f(\rho)$. This term was taken to be cubic $\rho(1 - \rho)(\rho - \rho^*)$. Once the calcium fades below the thresholds, ρ would be bi-stable, with stable states $\rho_\infty = 0$ and $\rho_\infty = 1$ and at tractor basin provided by unstable equilibrium ρ^* . In this model, synaptic strength is defined directly as the affine re-scaling of ρ from $[0, 1]$ to $[w_{min}, w_{max}]$.

However, the stochastic nature of the model is such that exact solutions can only be found by Monte Carlo, so that implementing this rule on a large network is computationally impractical. Our motivation was thus to investigate similar calcium-based models that would enable an implementation on a large-scale network. We chose a "top-down" type of modeling strategy: we looked at current knowledge in electrophysiology to try to better understand to what extent the model is biologically realistic, and through what modifications to it can one both stick to biological realism and produce a light-weight rule suitable for a neural network. To do this, we look at and synthesized a set of biologically detailed chemical models at the postsynaptic density. With this understanding at hand, we could then propose a simplification of the calcium-based model that would allow for large-scale deployment.

The next section introduces our work on biologically detailed models of postsynaptic plasticity.

Chapter 2

Detailed modeling of calcium-calmodulin based synaptic plasticity

The characterization of synaptic plasticity is the subject of a large corpus of literature. Among the most important questions that were the focus of the last several decades are the nature of synaptic weights (discrete number of states, vs continuum of possible states), the exact setting of plasticity (is it purely presynaptic, purely postsynaptic, or shared, with possible specialization of one site for potentiation while another takes care of depression) and key mechanisms responsible for plasticity (are they mostly chemical, structural or epigenetic?). These questions have only been answered in part, and a complete, accurate and universal picture of plasticity remains to be drawn, if it can be done. Let us first focus on the question of stability. There is not yet a strong scientific consensus as to whether the biological code at the synapse is discrete in nature, or if most synapses can stabilize at a continuum of efficacy values. One of the key reasons is that given neurons A and B , there are often a few hundreds direct synaptic connections $A \rightarrow B$. Moreover experimental constraints do not always provide clear answers at a very fine spatial scale. A series of experiments in synapses of the CA3-CA1 Schaffer collaterals (Malenka et al. 1988, O'Connor, Wittenberg, and S. S.-H. Wang 2005), suggest that the information stored at a single synapse is binary (the synapse is either 'ON' or 'OFF'), at least for this kind of synapses. This result is supported by several theoretical works showing that a bi-stable synapse would be more robust to the ongoing electric noise that it has to sustain (Higgins, Graupner, and Brunel 2014). However other recent studies refer to more than two possible synaptic states: John Lisman 2017 suggests quantal synapses with about ten different states.

To a large extent, the nature of the synaptic code would be linked to the mechanisms that drive plasticity. As it was introduced before, experimental scientists have identified different timescales at which synaptic plasticity takes place. Let us set aside what is called "short-term plasticity", and focus solely on LTP and LTD, which takes place on time scales of seconds to years. It is now well established that the first stages of long-term plasticity would be of chemical nature, and would involve mobilization and activation of various proteins and amino-acids at key locations of the synapse to modify the effective amount of post-synaptic current that follows a stimulus. Such chemical signaling would be responsible for the induction of synaptic plasticity. However, the storage of this information on time scales longer than hours would imply both chemical process (e.g the fixation of active calmodulin kinase protein II onto GluN2B subunits of NMDA membrane receptors) and structural changes of the synapse (enlargement of the postsynaptic terminal, restructuring of structural proteins inside the button, increase in number of available ion channels). Moreover, it is suspected that the chemical mechanisms that we deem responsible for the induction of plasticity trigger transfer of information from the postsynaptic button to the soma of the postsynaptic neuron, where gene expression is locally altered. In this way, epigenetics is increasingly considered as essential to plasticity maintenance on the time scale of days to years.

In this work we focus on chemical mechanisms that would be responsible for plasticity induction. We look at the issue of plasticity maintenance only in the sense that candidate mechanisms should allow the information to be retained for time scales of several tens of minutes, until mechanisms of different nature (structural, epigenetic) can take over.

2.1 Identifying mechanisms for plasticity induction

Several potential mechanisms for the induction of plasticity have been discovered and studied in the last decades. Some mechanisms take place mostly in the presynaptic spine and would involve for instance the greater mobilization of vesicles, as well as the phosphorylation of presynaptic VDCC. Other mechanisms of plasticity involve both the presynaptic and the postsynaptic side, like the propagation of retrograde messengers, such as endocannaboids (measured for instance in Cui et al. 2015) or nitrogen oxide, from the postsynaptic to the presynaptic terminal. Such messengers are of interest since they would allow for spike-timing dependent mechanisms to take place on the presynaptic side by increasing the probability of synaptic vesicle being released from the presynaptic side into the cleft, during later stimulation.

Conversely, some mechanisms are deemed to occur on the postsynaptic side only. One of the most popular hypothesis involved intracellular second messengers and protein kinase CaMKII. CaMKII is an oligomer that is transiently activated by calcium. It is a good candidate for encoding plasticity information in that it is regulated by calcium in an indirect fashion (through second messengers such as cAMP and PKA), and interacts with ion channels indirectly, playing a part in AMPA receptor phosphorylation (the ion channels become more likely to open in response to an incoming neurotransmitter, leading to larger EPSP on average) and exocytosis (new ion channels are inserted into the PSD, resulting in a larger pool of receptors to deliver larger EPSPs, faster).

Figure 2.1 provides a schematic representation of those two types of plasticity mechanisms.

Models of plasticity based on retro-messengers were recently investigated in Vignoud, Venance, and Touboul 2018. There is a good corpus of evidence for both retro-messenger-based and postsynaptic plasticity.

However, we mostly focus on purely postsynaptic mechanisms of plasticity, for four reasons:

- the CaMKII chemical pathway is deemed to be able to bring bistability to the synapse, and therefore this mechanism is theoretically crucial when investigating the nature of the synaptic code
- we needed to focus on one or a few mechanisms of plasticity, and a first study of other mechanisms did not seem to yield as interesting properties of stability as this one
- the base phenomenological model that we looked at (Graupner and Brunel 2012) claims to mimic the postsynaptic CaMKII pathway
- the postsynaptic pathway is sufficient to account for a wide range of experimental observations

To develop a simple model of how the synaptic strength evolves, we would need to answer the following questions:

- *What are the physical variables on the postsynaptic side that control synaptic strength?*
- *How do the second-messengers stemming from calcium influx interact with those physical ‘levers’ of plasticity?*

One of the main difficulties that we face in trying to answer those questions is that the network of chemical entities that interact with calcium ions is very large. Developing a good model of what happens would require to understand the kinetics of the reactions in this network of chemicals. Other challenges involve the fact that some key compounds are in low number at the post-synaptic density, and are not necessarily homogeneously spread. Indeed, the dense network of structural and transfer proteins on the postsynaptic side influences the speed of diffusion of many molecules. One can then see that any attempt to model the system of second-messengers must resort to simplifications: assumptions as to which compounds should be taken into account and which

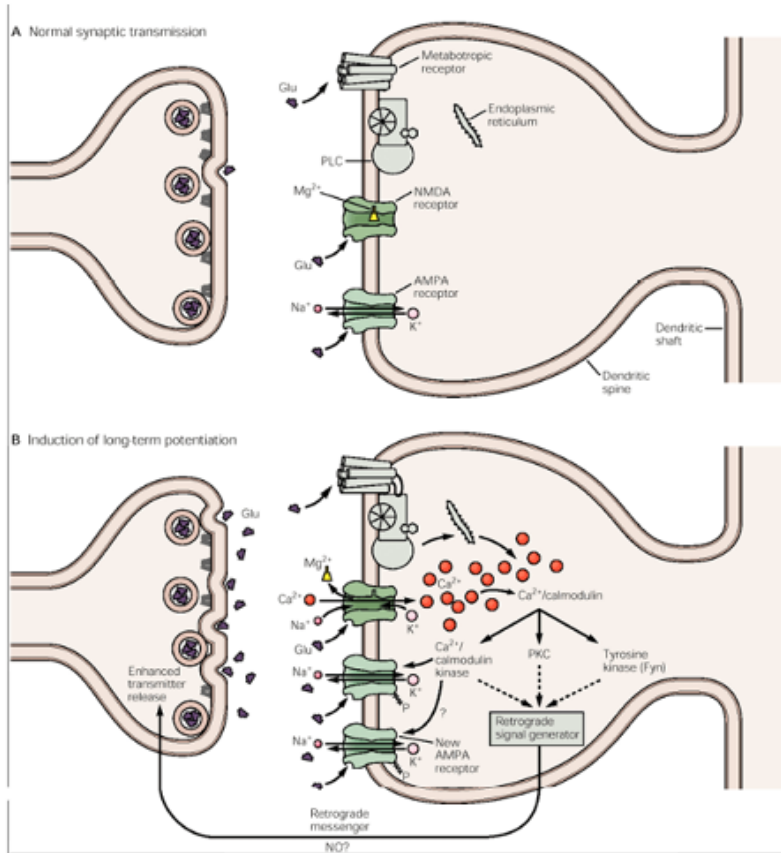


Figure 2.1: Schematic representation of two potential mechanisms of synaptic plasticity that can account for spike-timing dependency. **A:** Before stimulation, a synapse can be partly characterized by a given number of docked vesicles and a state for its associated trafficking proteins on the presynaptic side, and by a population of receptors and associated regulation and trafficking proteins on the postsynaptic side. **B:** A sufficiently strong stimulation (perhaps coordinated between pre and postsynaptic) caused the synapse to change in several ways. Calcium-based postsynaptic signaling and metabotropic receptors activation lead to activity of second messengers. Retro-messengers diffuse from the postsynaptic to the presynaptic side and increase the probability of vesicle release. On the postsynaptic side, cAMP and PKA second messengers cause both an increase in the number of available AMPA receptor at the membrane and an increased propensity for the existing AMPA receptors to open. Courtesy of Kandel & Schwartz, **Kandel**

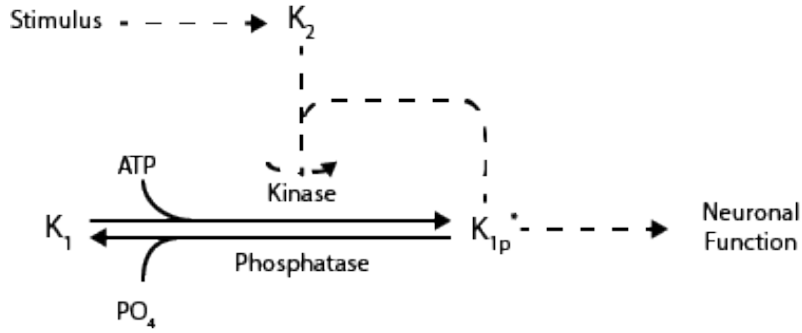


Figure 2.2: Mechanism proposed by Lisman (1985) for a bi-stable chemical switch. The concentration of phosphorylated kinase K_1^P provides the switch level. Kinase K_1 can itself undergo kinase at a variable speed that depends both on the action of kinase K_2 and on the concentration K_1^P through a process known as autophosphorylation

compounds we should ignore, the use of punctual models even though the system has a well-defined spatial structure with compartments, etc. The spatial location of molecules may only be important in some cases, and so one must be careful as to when a spatial model is necessary (to account for cytoplasmic or intra-membrane diffusion, or to account for variable concentrations at the PSD and far into the cytoplasm) and when such complexity is superfluous.

Synaptic modeling has, from the start, used experimental results to both posit mechanisms and test model predictions. It will then be to no surprise that a lot of modeling efforts have followed experimental results that concluded to the digital nature of information at the synapse. A fundamental paper by John Lisman (J. E. Lisman 1985) proposes a mechanism by which protein kinases can implement a bi-stable chemical switch in cells. Kinases are proteins that are capable of activating various compounds by adding a phosphate group to them, by reacting with Adenosine TriPhosphate (ATP)¹. More recently, Urakubo et al (Urakubo et al. 2008) confirmed the bistability of this mechanism in vitro. All that would be necessary to implement this switch would be two protein kinase that interact with one another according to Fig 2.2. The key mechanism of the switch is the combined effect of K_2 on the activation of K_1 and the positive feedback effect of the activation of K_1 through autophosphorylation. Note that the kinase and phosphatase (the excitation and inhibition mechanisms of K_2 onto K_1 , respectively) are versatile mechanisms used by proteins to activate and deactivate one another in biological systems.

The Lisman lab, next door to ours, studies such molecular mechanisms, with a specific focus on protein CaMKII, that is deemed to be of tremendous interest in many cellular biology, and in particular at the synapse. Their work (Lisman 1989, John Lisman, Schulman, and Cline 2002, Shifman et al. 2006) has led to a better understanding of the role of this complex protein.

2.2 Calmodulin-dependent protein kinase II and its role in synaptic plasticity

2.2.1 Calmodulin-dependent protein kinase II

Calmodulin-dependent protein kinase II, usually abbreviated to **CaMKII**, is a structured protein that is deemed to be both ubiquitous and of prime importance in cellular mechanisms of many cell types. CaMKII constitutes approximately 2% of proteins in the brain, and is especially present at postsynaptic spines. It is an holoenzyme, a compound made out of twelve identical sub-units grouped into two rings of six sub-units, stacked together. Its structure is described on fig 2.4A.

Fig 2.4C provides a description of one single sub-unit. The protein structure of a single sub-unit can be established as follows:

- the **hub** region is the part of the sub-unit that binds it to other sub-units of the same ring

¹The reaction is also called kinase. Protein kinase is considered to be an enzyme in this reaction

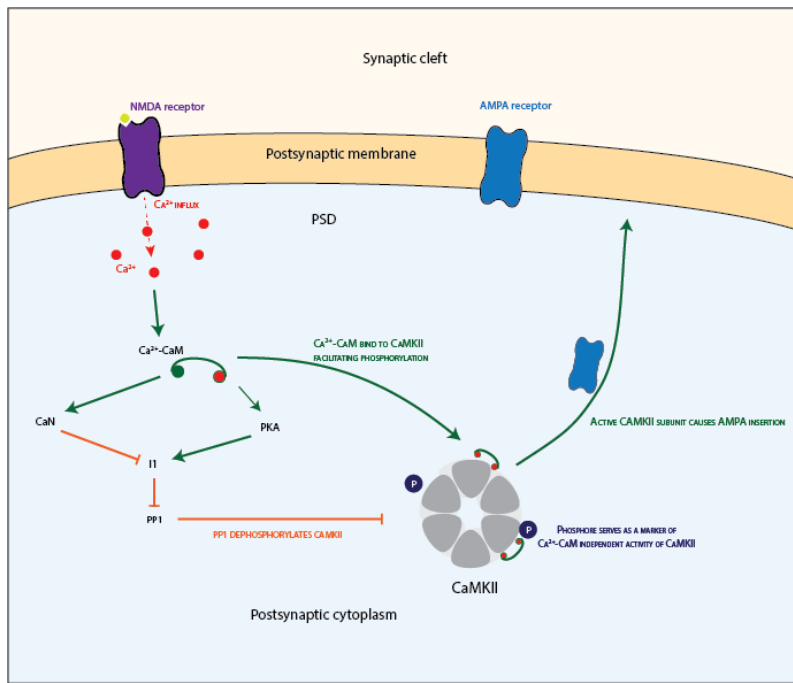


Figure 2.3: Representation of the second-messenger pathway stemming from post-synaptic calcium, resulting in the insertion (or exocytosis) of AMPA receptors in the PSD, effectively increasing the synaptic strength. Following a presynaptic spike, and as soon as NMDA channels can open, Ca^{2+} ions will flow into the postsynaptic cytoplasm, close to the PSD. Second-messenger molecules (CaM, PKA, I₁, PP1, CaMKII) will then be activated by calcium. Green arrows indicate excitatory action (inputs are either reactants or catalytic enzymes), orange arrows ending with a bar indicate inhibitory action. Second-messengers in turn control the activity level of Calmodulin-dependent Protein Kinase II (called CaMKII) both in an excitatory and in an inhibitory manner, with a net action that depends on the exact concentrations involved. Note that a similar action of AMPA removal (or endocytosis) can be led by protein phosphatase 1 (PP1), such that the history of calcium concentration as well as the state of other parameters can determine if there is net addition or removal of receptors into the membrane. In turn, the relative levels of CaMKII and PP1 activity is a good predictor of the net insertion or removal of AMPA channels.

- the **linker** region can vary in size in response to calmodulin binding to the sub-unit, effectively regulating the availability of the sub-unit to further activation
- the **regulatory segment** (or pseudo-substrate) is the site of the sub-unit where calmodulin can bind and where the Threonine-286 and Threonine-305/306 lie

As seen further, these sites play crucial roles in the sub-unit activation. By looking at the states of such site, we can effectively design a model of CaMKII, as introduced further.

Each sub-unit can interact with calcium-bound calmodulin (Ca^{2+} -CaM), protein kinase A (PKA), calneurin (CaN), and can be phosphorylated by another sub-unit of the same ring in a process called autophosphorylation. Such interactions are described a bit further down.

2.2.2 Pathway leading to CaMKII activation

Figure 2.5 introduces a simplified version of the pathway that we will refer to here as the "calcium-CaMKII pathway". The compounds described in the figure in black all exist at basal state in the postsynaptic button. They are all activated in some way depending on calcium concentration. The second messenger that both comes first and is common to all further messengers in the chain of causality is called **calmodulin**. Calmodulin is a protein with a tertiary structure that makes it look like a hairpin. The molecule has two lobes that can each capture two Ca^{2+} ions (see Faas et al. 2011). As they capture calcium ions, they become capable of binding to several functional proteins in the cell, among which CaN, PKA and CaMKII proteins (Shifman et al. 2006).

There are three important things to note about the pathway of activation of CaMKII:

- it effectively fits the conceptual framework of bi-stable switch introduced by Lisman in J. E. Lisman 1985. CaMKII embodies the switch, while calcium-bound calmodulin acts as K_2 .
- the phosphatase activity is itself dependent on the level of calcium-bound calmodulin, through the competitive excitation of phosphatase via CaN and inhibition via PKA. This double control of CaMKII is the key to an important property of CaMKII activity. Concurrent phosphatase activation and deactivation has been studied and laid out by experimental studies (see Li, Stefan, and Le Novère 2012).
- autophosphorylation is the process that provides positive feedback onto phosphorylation of CaMKII sub-units (see Blitzer et al. 1995). Suppose that a unit is bound to Ca^{2+} -CaM. It can react with the sub-unit lying directly next to it (only in, say, the clockwise direction), and add a phosphate group at the T-286 site of this neighbor. This makes the neighbor subunit active in a manner independent on the presence of Ca^{2+} -CaM. Autophosphorylation can occur whether or not the Ca^{2+} -CaM bound unit is itself phosphorylated at T-286. Also note that the source sub-unit does not lose its activity in the process (instead one molecule of ATP reacts into ADP).

Because of the structure of this pathway, CaMKII is deemed to implement the bi-stable switch described in J. E. Lisman 1985. Fine-grain models of CaMKII activation also conclude to its bi-stability in at least part of the range of realistic parameter values. Experimentally, CaMKII has been found to be bi-stable in some cases and for a duration that could match the induction of synaptic plasticity. Some subtleties and details have to be taken into account, for instance additional conditions on CaMKII for its activation to sustain in time (e.g binding to NMDA receptors is necessary for maintenance of the information past minutes; see Bayer et al. 2001 and He, Kulasiri, and Samarasinghe 2015).

2.2.3 Action of CaMKII on synaptic strength

CaMKII activity has been shown to be both necessary and sufficient to the induction of LTP (John Lisman, Schulman, and Cline 2002, Rossetti et al. 2017). Once sub-units of CaMKII are activated, either by phosphorylation or by calmodulin, they can in turn activate other proteins that have an effect on synaptic strength:

- By phosphorylation of AMPA receptors (see figure 2.9, and J. Q. Wang et al. 2005 for a review of the mechanism). Phosphorylated AMPA receptors have an increased probability to open "wider" in response to neurotransmitter binding from the cleft.

- By activating action (stargazin) and scaffold protein (PSD-95 complexes), CaMKII sub-units can cause changes in the effective number of AMPA receptors available at the PSD. There are two mechanisms posited to play a role in altering synaptic strength:
 - AMPA receptors exocytosis and endocytosis, caused by insertion or removal of active AMPA receptors to or from the membrane (Bredt and Nicoll 2003, Collingridge, Isaac, and Y. T. Wang 2004). Those membrane receptors can be added directly onto the PSD, but also farther away from the active site, for instance on the sides of the postsynaptic button, or even on the dendrite
 - AMPA receptors lateral diffusion through the membrane. Many membrane molecules are deemed to be moving within the membrane quite intensely, unless "anchored" to a specific location by a specific process. This lateral diffusion occurs intensely in vivo. Moreover, it was found that this diffusion is actively regulated at synapses by compounds that are activated by CaMKII. Stargazin is thought to be phosphorylated by CaMKII and to interact with structural proteins near the membrane to "trap" AMPA receptors (Tomita et al. 2005, Opazo et al. 2010, Constals et al. 2015). The reason why trapping can affect the EPSP size is a phenomenon called receptor deactivation. Once a receptor activates following arrival of neurotransmitter, it will close and remain in a deactivated state for some period of time. Receptor trafficking would allow for the synapse to respond to high-frequency stimuli without saturation. By indirectly controlling the trafficking of receptors, CaMKII could in effect change the size of EPSPs.

2.2.4 Modeling CaMKII activation

Because of the theoretical interest of CaMKII, a large effort was spent in the last decade to model CaMKII in a way that could account for experimental data.

As part of our investigation as to how calcium influx leads to changes in synaptic strength, we investigated one of these models of CaMKII activation. A landmark model of CaMKII activation was developed by Zhabotinsky in 2000 (Zhabotinsky 2000) and showed how the protein can be the bistable switch that Lisman hinted existed in J. E. Lisman 1985. With more up-to-date knowledge of the molecular processes at play, Graupner and Brunel furthered his model in 2007 (Graupner and Brunel 2007). The updated model uses the available knowledge on the kinetics of the "Ca²⁺-CaMKII" pathway, and makes several assumptions in order to conclude on the behavior of CaMKII phosphorylation level (ie the concentration of CaMKII sub-unit that are "independent active").

In the model, a sub-unit can be in one of four states:

- self-inhibited (non-bound, unphosphorylated) D_u
- CaM-dependent active (Ca^{2+} -calmodulin bound, unphosphorylated) C_u
- Doubly active (Ca^{2+} -calmodulin bound, phosphorylated) C_p
- CaM-independent active (non-bound, phosphorylated) D_p

The concentration of CaMKII sub-units in each state, noted $[D_u]$, $[D_p]$, $[C_u]$, $[C_p]$ and the concentration of the different states of CaMKII holoenzymes, noted $(S_i)_{i=1..13}$ are interdependent. This dependency results in lack of knowledge of one of the reaction rates involved in CaMKII phosphorylation. In short, because different holoenzyme states have different geometries and transfer to one another at different speeds, **at least one reaction constant depends on the concentrations of all states of holoenzyme**. The system can nevertheless be solved explicitly under some assumptions that were made in Graupner and Brunel 2007. In appendix A we question this assumption and look at ways to solve the general system, which requires implicit integration.

The equations for the model are provided in appendix A. They are mostly derived from chemical kinetics (law of mass-action, Michaelis-Menten reactions, ...). The main trick in this model is that **its dimension can be greatly reduced**. In this model, we consider that the two rings constitutive of an holoenzyme do not interact with one another. We can therefore look at holoenzymes made of a single ring a six sub-units. Based on the fact that many different states of such a six-units ring can be identified to one another through rotations and symmetries, we are left with 13 states for a CaMKII holoenzyme. Figure 2.8 provides a description of these states, as well as the graph of transitions between one state to the other.

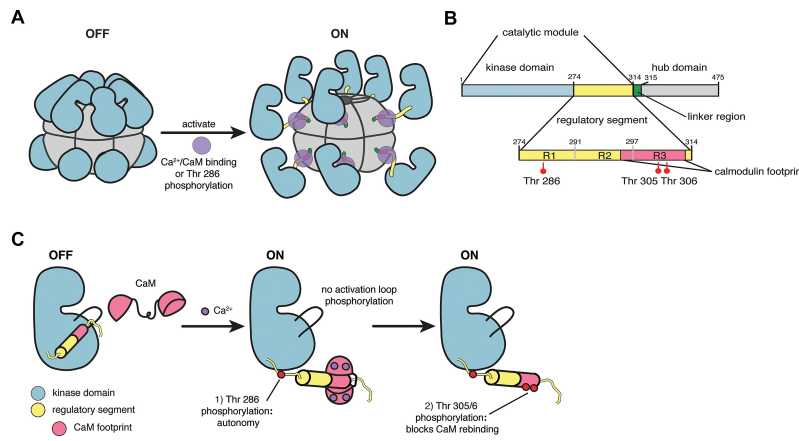


Figure 2.4: Schematic representation of a calmodulin-dependent protein kinase II (CaMKII) holoenzyme. The holoenzyme is composed of two groups of six sub-units in an hexagonal configuration. The behavior of a sub-unit can be mediated in several ways. **C-1:** In its inactive state, the sub-unit has its kinase site (blue) obstructed by a regulatory segment, which keeps it in the inactive state. **C-2:** Binding of Ca^{2+} -CaM at the regulatory segment causes it to lie outside of the active region, leading to its activation. While Ca^{2+} -CaM is bound to our sub-unit, the regulatory segment let bare can phosphorylate the neighbor sub-unit at its Threonine-286 site in a process called **autophosphorylation**. **C-3:** While phosphorylated, the sub-unit remains active even once the Ca^{2+} -CaM is removed. Action of protein phosphatase (such as PP1) is then required to deactivate the sub-unit

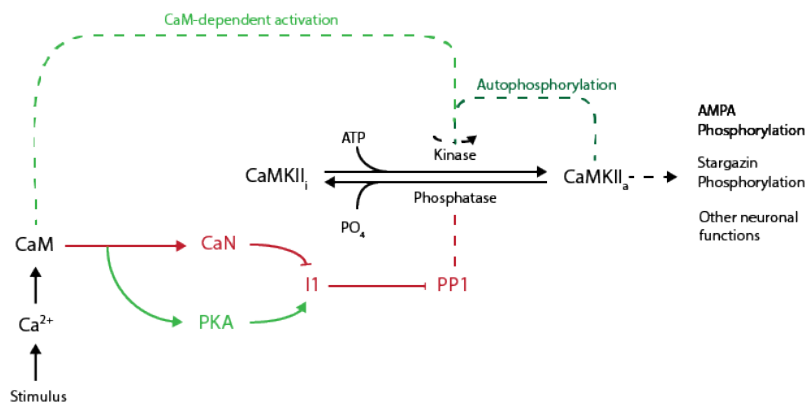


Figure 2.5: Representation of chemical pathways in the model of Graupner and Brunel, effectively fitting the theoretical framework from J. E. Lisman 1985

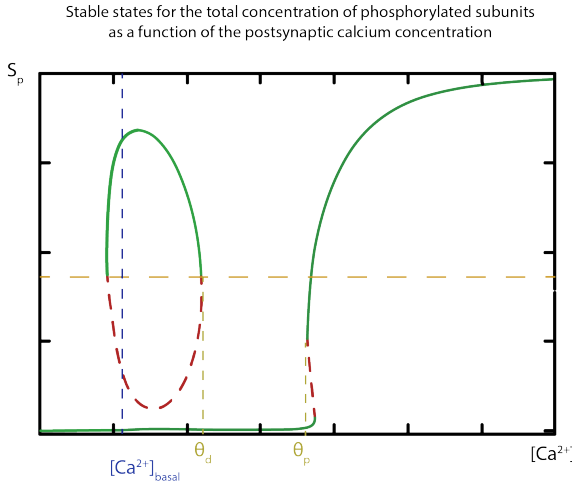


Figure 2.6: Bifurcation diagram providing the stable states of the concentration of phosphorylated CaMKII sub-units as a function of the concentration of calcium in the postsynaptic spine. At basal concentration (dotted blue line), there are two stable activation states: a 'LOW' state corresponding to a low concentration of active sub-units, and a 'HIGH' state. During excitation of the synapse, the calcium concentration rises from the basal concentration, which can lead the system to change of stability, and to effectively evolve towards a different concentration of phosphorylated sub-units. The final state of the system once calcium sets at its basal level depends on the history of the system, namely on its trajectory relatively to the basins of attraction of each stable state

The relevant quantity in this regard is the concentration of active CaMKII sub-units. Of course, one must note that sub-units always come in rings of six. One simplification that is implicit to the model of Graupner and Brunel is that we can just consider each ring as six (spatially and functionally) independent sub-units as far as we look at their action on second-messengers that lie downstream on the pathway to plasticity. We therefore consider the total concentration of phosphorylated sub-units:

$$S_p = \sum_{i=1}^{13} m_i S_i$$

Here m_i is the number of phosphorylated sub-units for holoenzyme state S_i . More specifically, we are interested in the stable states of S_p for this model. Graupner and Brunel 2007 has led such a study using software XPPAUT (Ermentrout 2000–2016). They found that **at basal calcium concentrations** (meaning the concentration within the postsynaptic cytoplasm in the absence of calcium influx), S_p is bi-stable (see fig 2.6)

A bifurcation diagram (see Fig 2.6, and Strogatz 2000 for an introduction to these diagrams and to dynamical systems) is a way to visualize the stable state of the system as a function of parameters. Here the calcium concentration is looked at as a parameter of the system. The bifurcation diagram presents several interesting features:

- A lower branch presents two fold bifurcations at high calcium concentrations. This leads to a narrow range of calcium at which two states are stable (in green), with a third unstable state (in red) that defines the limit of the basin of attractions of the two stable states. As this bi-stability exists only over a narrow range of calcium that is much higher than basal level, the bi-stable range is usually overlooked, and we focus instead on the transition from a low phosphorylation state (before θ_p) to a high state (after θ_p)
- An upper branch of the diagram forms an "egg" at low calcium concentrations, including basal calcium concentrations. This egg can better be seen and interpreted in co-dimension 2. It is a cusp bifurcation, which implies that the egg does not effectively exist for all values of other parameters. However, at most basal values of parameters, this egg exists, and implies that there are two stable states at rest concentrations of calcium.

In a sentence, the CaMKII system that stems from this model can tell us how CaMKII activity depends on the history of calcium influx into the postsynaptic spine. This is very useful if we assume that we can then somehow map CaMKII activation to synaptic strength. I will introduce some of our efforts to model this link afterwards.

Let us first understand how a given history of calcium influx influences the activity of the system. Because the calcium concentration in the postsynaptic cell is fixed and known at rest, the activation level at rest must be at the intersection of line $[Ca^{2+}]$ with the bifurcation diagram at one of the two steady states. Because the "egg" includes the basal calcium concentration, there are indeed two possible states for CaMKII activity at rest ('UP' and 'DOWN').

Now let's assume that through a stimulus we make calcium flow into the postsynaptic spine. $[Ca^{2+}]$ will increase. If the influx is high enough, the activity level may start to change. The bifurcation diagram introduces two important thresholds that affect its behavior:

- a **potentiation threshold** θ_p . The only stable state for CaMKII activity above that threshold is high, which implies that if $[Ca^{2+}]$ rises above that threshold, the system will be driven towards the high stable state. If we were to maintain calcium concentration above the threshold long enough, the system would eventually stabilize at this high state of activity
- a **depression threshold** θ_d , with $\theta_d < \theta_p$. The only stable state between those two thresholds is low activity, which means that by sustaining calcium concentration at a level between the depression and the potentiation threshold for long enough, the system will eventually stabilize itself at a low CaMKII activity level.

This can help us see how activity responds to $[Ca^{2+}]$. Based on this concentration at a given time, the system will increase or decrease its activity. Because calcium concentration eventually needs to come back to its basal level, the system will eventually stabilize at a stable state for basal concentration. Which states ('UP' or 'DOWN') it ends up in depends on the relative amount of time spent above θ_p and between θ_d and θ_p , as well as on the rate of change of phosphorylation level as a function of calcium concentration. Figure 2.7 provides an example of the response of the system in terms of activity level, as a response to two different calcium stimuli, a short one and a longer one. Even though the activity levels are initially the same, the activation level can take different paths over time, since both the direction and the rate of change depend on calcium concentration which may differ at many points in time. Eventually, concentration will come back to the basal level, at which point the system can be in a sensibly different state of activity. The red dotted lines in 2.6 indicate the limit of the basin of attractions for the stable states. Whether the system ends up on one end or the other of this limit tells us what its final value will be, once it has been given enough time to converge to the "closest" stable state (as defined by the basin of attraction).

Let us note that even though we only focus on the activation (ie phosphorylation) level, the system is in 14 dimensions. The key idea is that the activation level (which in itself is a linear combination of these 14 variables) is bi-stable at basal calcium. This does imply that all 14 variables have at most two stable states at basal calcium concentration, but some of them may well be mono-stable... The stability of each variable can be investigated using XPPAUT, and we cover some of this analysis in appendix B.

2.2.5 Modelling synaptic strength as a function of CaMKII activation

CaMKII is a versatile protein that activates many other proteins, generally by using one or more of its active sub-units to phosphorylate a target protein, leading to its activation. There are several downstream pathways that are deemed to be responsible for modulation of synaptic strength. I will describe some of them in a chronological order of discovery and level of focus from the community.

direct phosphorylation of AMPA receptors which are the membrane receptors that can respond to unilateral stimulation by letting Na^+ into the postsynaptic spine, leading to its depolarization. The conductance of each single channel contributes to the size of the EPSP when a presynaptic stimuli reaches the synapse. AMPAR open and close in response to neurotransmitters arriving from the cleft in a probabilistic manner. They can be in one of four conductance states, the lower corresponding to a "closed" channel, and the higher corresponding to a fully open channel. AMPA receptors are made out of four sub-units, some of which (GluR4) can be phosphorylated by active sub-units of CaMKII. Once phosphorylated,

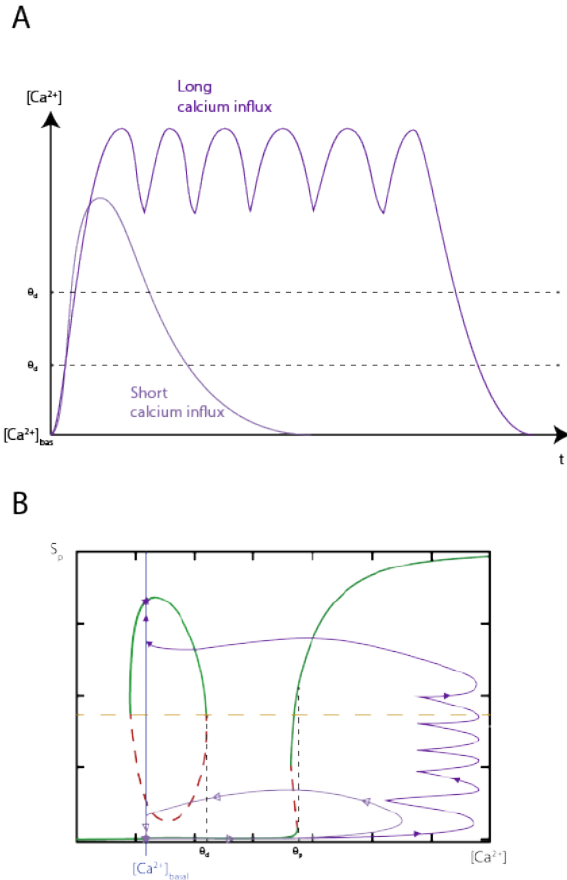


Figure 2.7: Evolution of CaMKII activity in the model of Gruapner & Brunel 2007 in response to two different histories of calcium influx into the postsynaptic spine, for a same initial state. **A:** Two calcium histories. The light purple curve shows a short single impulse of Ca^{2+} ; while the dark purple curve shows a longer history caused by the summation of several consecutive impulses. The dark purple calcium is sustained for a longer period of time above the potentiation threshold θ_p relatively to the time it spends above the depression threshold θ_d . **B:** evolution of the total CaMKII activation level, plotted in the codimension-1 bifurcation diagram of parameter $[Ca^{2+}]$. Note that when $\theta_d < c(t) < \theta_p$, the concentration of active units is driven downward, whereas it is driven upwards when $\theta_p < c(t)$. Stars indicate the two possible stable states, at the intersection of the basal calcium level (vertical dotted line) and the bifurcation diagram

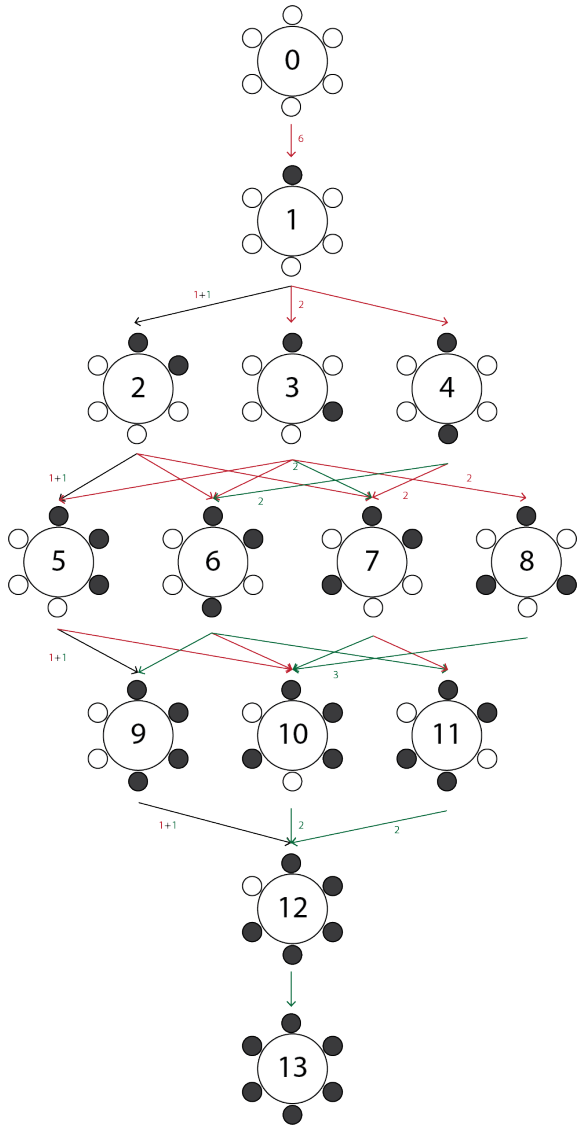


Figure 2.8: Graph of the transitions between the different states of CaMKII holoenzymes. Knowledge of this graph, the reactions involved and their kinetics leads us to the equations of the detailed model. Each possible state is represented by a number within a circle, surrounded by six smaller circles representing the state of each sub-unit of a ring. A filled circle means a sub-unit phosphorylated at its T-286 site. Once we identify states through symmetries and $\frac{\pi}{6}$ rotations, we come down to 13 states for a six-units ring. Each line corresponds to a different number of phosphorylated sub-units (between 0 and 6). Arrows indicate the possible transitions between the states, due to chemical phosphorylation of a sub-unit (dephosphorylation reactions are omitted here). Red and green arrows indicate different reactions (with different kinetics). Atop each arrow is indicated the number of reactions of each type that lead to the downstream state.

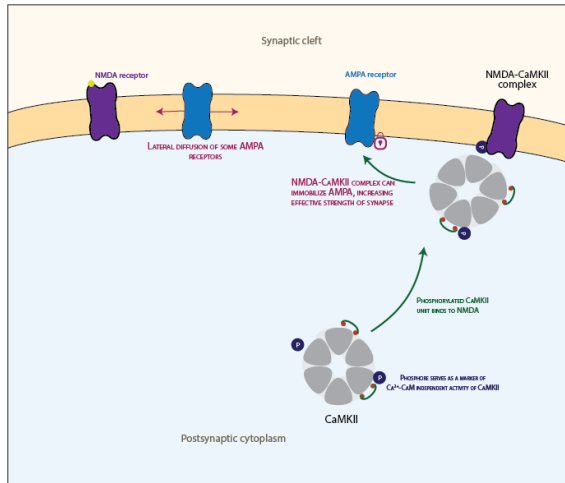


Figure 2.9: CaMKII holoenzymes are composed of a pair of six units that can both bind to calmodulin and be phosphorylated. These events cause activation of the specific sub-unit, that can in turn perform a wide range of task. In particular, the sub-unit can bind to a NMDA channel from the PSD, where it can then act on AMPA receptors, allegedly by slowing down their lateral diffusion through the membrane, increasing the effective conductance of the postsynaptic membrane

AMPAR have a higher probability of switching to higher conductance states when neurotransmitters are captured. This leads to the effective modulation of synaptic strength by CaMKII

exocytosis and endocytosis as explained in previous section

lateral diffusion as explained in previous section

The action of stargazin and of PSD-95 on the retention of AMPAr at the PSD is interesting, since it is a complex mechanism, which could react in a graded manner. In this way, this mechanism could very well transmit the bistability of CaMKII and make the synaptic strength bimodal, which is close enough to bi-stable. However, the exact interaction of CaMKII, stargazin, other action proteins and scaffold proteins within the cytoplasm and at PSD is not well understood, and focusing on a model of such interactions would be pointlessly uncertain.

Phosphorylation and receptor exocytosis are both simpler phenomena to model, even though experimental data suggests an important role for receptor diffusion within the membrane. A model of receptor phosphorylation that we developed and implemented is introduced in appendix B. The model is helpful to see how CaMKII activity would translate in terms of synaptic strength.

2.2.6 Simulation of the evolution of phosphorylation under minimal assumptions

The model developed by Graupner and Brunel concludes to bistability of the total concentration of phosphorylated subunits of CaMKII, which has a theoretical appeal to one who directly equates CaMKII phosphorylation and synaptic strength. However we must make two important remarks:

- the mechanisms that CaMKII can use (phosphorylation, exocytosis of AMPAr, their immobilization through scaffold proteins) have no reason to be linear, and the synaptic strength of the synapse is not necessarily bistable itself
- To conclude to bistability at basal calcium level, Graupner and Brunel have made several assumptions that constitute limitations to what they can conclude.

Altough many assumptions must be made to conclude to anything in such models, the authors of Graupner and Brunel 2007 made three main assumptions that, according to us, are questionable and that can qualitatively change the behavior of the system when dropped.

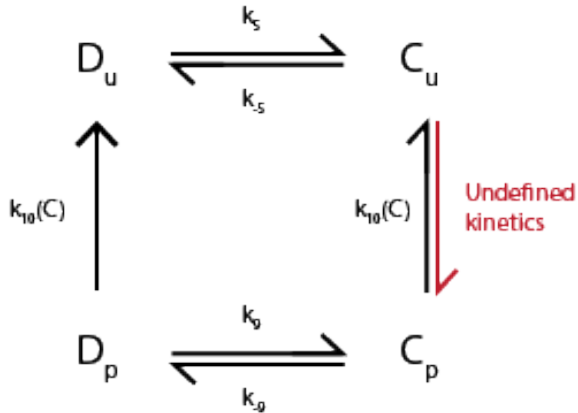


Figure 2.10: Graph of the different CaMKII sub-unit states and their transitions in the model of Graupner & Brunel 2007. The exact kinetics of $C_u \rightarrow C_p$ depends on the concentrations of the different states of CaMKII holoenzymes, and cannot be enunciated. Each sub-unit can be bound to a calcium-calmodulin and/or phosphorylated at its T-286 site, leading to four possible states per sub-unit.

Constant available calmodulin Two quantities are especially important in the model:

$$\gamma(t) = \frac{C_u}{D_u + C_u}$$

the fraction of T-286 unphosphorylated CaMKII subunits that are bound to calmodulin

$$\gamma^*(t) = \frac{C_p}{D_p + C_p}$$

the fraction of T-286 phosphorylated CaMKII subunits that are bound to calmodulin

Those variables determine the kinetics of formation of the different states of CaMKII complex. When calcium-bound calmodulin is assumed to be constant, meaning that throughout the simulation the calmodulin that is made active by calcium is fully available to bind to CaMKII, the two quantities γ and γ^* can be obtained directly at each time step. However, when this assumption is dropped, γ and γ^* become the solutions of a system of equations of order 4 that is harder to solve. The equations that govern the whole system become stiff, therefore being much harder to solve...

We have produced simulations of the system when the assumption of constant available calmodulin is relaxed. Our simulations (see 2.11) seem to indicate that relaxing the constant available calmodulin hypothesis does not invalidate bistability. 2.11 shows a case in which the system start in a 'DOWN' state (most CaMKII subunits are inactive) and end up in an 'UP' state (most CaMKII subunits end up independently active). Other simulations of ours show systems starting and remaining in their initial excitation state, or system switching from an 'UP' state to a 'DOWN' state, in response to less intense and equally prolonged calcium influx.

No phosphorylation at threonine-305/306 sites CaMKII subunits can not only be phosphorylated at their threonine-286 site to become calmodulin-independently active. They can also be phosphorylated at the threonine-305 and threonine-306 sites. This is only possible if the subunit was bound to calmodulin before, and the calmodulin has detached from the subunit, leaving bare the T-305 and T-306 sites. When phosphorylated at T-305 or T-306 (often considered to be one single site T-305/ 306), the subunit can no longer bind to calmodulin, until the phosphate group added at the 305/306 is removed (see Hell 2014). In Graupner and Brunel 2007, Graupner and Brunel chose to ignore the role of T-305/306. One of the reasons for doing this is that considering those sites, one must add additional subunit-level states to the model, which results in increased complexity. However, authors such as Michalski (Michalski 2013) have simulated the evolution of the system with the constant calmodulin assumption but taking into account the T-305/306 sites.

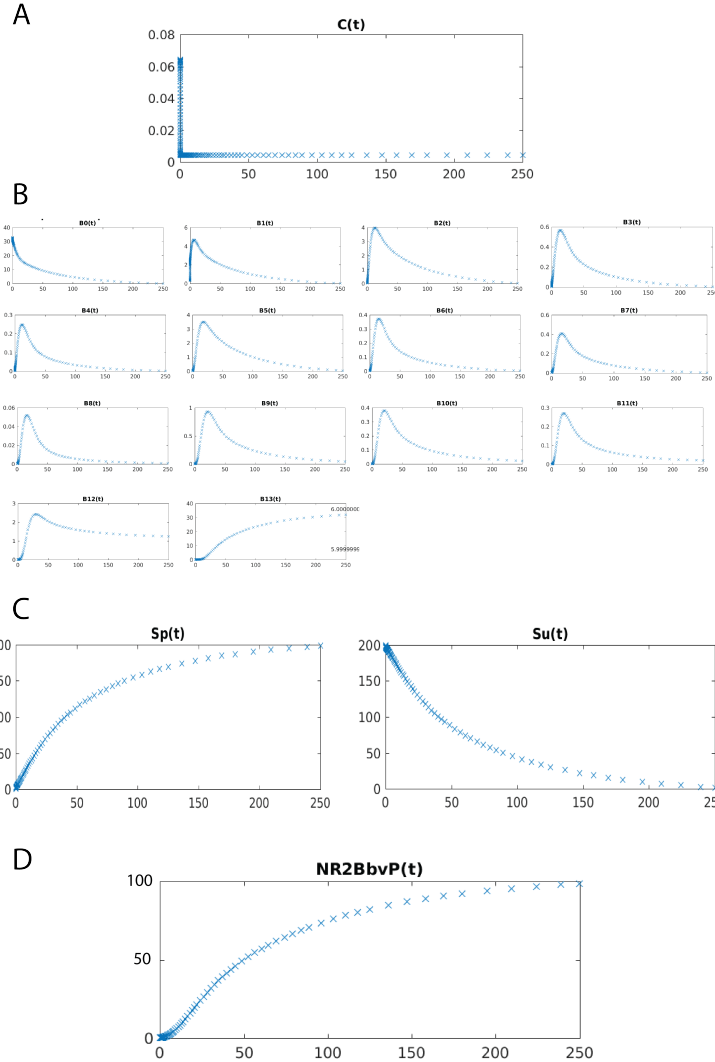


Figure 2.11: Evolution of the system for 250s in response to a burst of calcium of less than 1s at about $5\mu M$. Note that the system has multiple time scales: calcium is evacuated from the postsynaptic cell in the time scales of hundreds of milliseconds, while the evolution of phosphorylation is on time scales of seconds to hundreds of seconds. **A:** the burst of postsynaptic calcium that triggers the change of state of the system. **B:** evolution of the concentration of CaMKII complexes in different activation state, each defined by 2.10. **C:** evolution of the total concentration of phosphorylated (left) and unphosphorylated (right) CaMKII subunits with time. In this case, the burst of postsynaptic calcium was important enough so that the system stabilizes in a high phosphorylation state, where almost all CaMKII subunits end up phosphorylated. **D:** evolution of the number of CaMKII subunits that are bound to subunit BluN2B of the NMDA receptors at the postsynaptic membrane. This quantity is important since only CaMKII that are bound to NMDA receptors can remain phosphorylated for hours after the calcium concentration has faded. Once bound to NMDA receptors, the phosphorylated subunits of CaMKII that are free of movement can phosphorylate AMPA receptors or interact with scaffold proteins and stargazin to control the trafficking and trapping of AMPA receptors at the PSD. In these simulations, the total available calmodulin is set at $10\mu M$, the total concentration of CaMKII subunits is set at $33\mu M$. The parameters and other initial concentrations were taken to be the same as in Graupner and Brunel 2007

The number of subunit states goes from 4 to 6. The number of possible holoenzyme configurations comes up remarkably. Using a probabilistic method of simulation (Gillespie), Michalski showed that in general, **CaMKII is not bistable at basal calcium concentration levels**.

We intended to simulate the evolution of the system in the general case where the concentration of available calcium-bound calmodulin is made able to vary, and where T-305/306 phosphorylation is taken into account. The resulting system is however extremely complex to simulate, for the following reasons:

- the differential equations are stiff
- the system of equations is split between ODEs and Differential Algebraic Equations. Most solvers do not handle mixtures of stiff ODEs and DAEs, so we had to alternate between a step of integration of stiff ODEs and integration of the DAEs. This method allowed to simulate longer times, but the system still ends up to be unstable, and we were not able to reach any solid conclusion. It would seem that the system reached a singular states, beyond which we can no longer integrate. Collaboration with a person more expert in numeric schemes and integration may unblock the situation...

We provide the equations of the general system in appendix B, as well as a schematic description of the subunit states.

Conclusion of the study of fine-grain models Our main motivation for looking at fine-grain, biologically inspired models, was to understand how we could develop a phenomenological model that would enable us to simulate a single synapse through a few equations, without the need to run many simulations to compute estimates of random quantities (as this is really the part of Graupner and Brunel 2012 that makes it impractical for implementation in a network). We turned to models of the CaMKII pathways that led us to understand that under some assumptions, but for most plausible values of parameters, the concentration of activated CaMKII subunits implements a bistable switch at the postsynaptic spine.

We explored the details of Graupner and Brunel 2007 and Michalski 2013 to understand the limits of validity of this bistability. We were precluded from a strong conclusion as in the general case the system is hard to integrate. We did, however, question the transmission of bistability from CaMKII activation to synaptic strength (only on the postsynaptic side), as defined by the spatial distribution of AMPA receptors at the PSD and the expected conductance of those receptors in response to a given load of neurotransmitters from the cleft.

When studying the bifurcation diagram of the model by Graupner and Brunel (2007) in the $(S_p, [Ca^{2+}])$ plane, we did find interesting ways to look at a trajectory, so that a phenomenological model that would not need Monte-Carlo could be developed and studied. This led us to use the knowledge from our study of fine-grain models and to come back to the design of a phenomenological model...

Chapter 3

From a detailed to a phenomenological model

We have seen in the previous chapter how modeling of protein CaMKII can provide an hypothesis as to the bistability of CaMKII, and why the transfer of this bistability to synaptic strength is non-trivial and unestablished. The mere complexity of the system both in number of different compounds, in size, in spatial effects, noise-induced effects, etc is the main element that precludes us from producing any reliable conclusion on synaptic strength.

In general, complexity of a biological system constitutes a barrier to any fine-grain modeling of the system. The number of parameters that are involved are often astronomical, and those parameters are often not known up to one or more orders of magnitude of their expected value, mainly because we do not have the technology to assess their value experimentally.

This motivates another approach to modeling synaptic plasticity, and to modeling biological systems in general. A more goal-oriented approach to modeling would be to focus on a few features of the system, and to create a coarse model that tries to emulate the behavior of the system while remaining computationally simple. Those models are called phenomenological models, and generally consist of a few equations and parameters, so as to remain easy to both simulate and tune.

Such models can come short of offering interpretable results or parameters, since they try to mimic the behavior of a system without necessarily being built on biophysical quantities and processes. Some, however, avoid this shortcoming and allow for both efficiency and accessibility as far as interpretation. I will start by introducing such a model, created by Graupner & Brunel in 2012 (Graupner and Brunel 2012).

This is a calcium-based model, meaning that it stipulates that synaptic strength is acted upon by calcium concentration. Given a calcium history, one can use the model to find out how the synaptic strength would evolve.

The input to our model should however not be the calcium history itself, but a sequence of presynaptic and postsynaptic spikes; this way we can simulate the behavior of a synapse directly as a function of the activity of the presynaptic and the postsynaptic neurons. What this means is that we also need an equation that provides the postsynaptic calcium as a function of both the presynaptic and postsynaptic neurons activities.

The system therefore has two equations: one for the postsynaptic calcium concentration c and one for the phosphorylation level ρ , which is assumed to map directly to a synaptic weight w through an affine relationship.

$$\tau_c \dot{c} = -c + C_{pre} \sum_{i \in I} \delta(t - t_{pre}^{(i)}) + C_{post} \sum_{j \in J} \delta(t - t_{post}^{(j)} - D) \quad (3.1)$$

$$\tau_\rho \dot{\rho} = \rho(1 - \rho)(\rho^* - \rho) + \gamma_p(1 - \rho)\Theta(c(t) - \theta_p) - \gamma_d\rho\Theta(c(t) - \theta_d) \quad (3.2)$$

$$+ \sigma \sqrt{\Theta(c(t) - \theta_p) + \Theta(c(t) - \theta_d)} \eta(t) \quad (3.3)$$

Equation 3.1 provides the behavior of postsynaptic calcium. Assume a synapse $A \rightarrow B$, with presynaptic spike history $(t_{pre}^{(i)})_{i \in I}$, and postsynaptic history $(t_{post}^{(j)})_{j \in J}$. When a presynaptic spike

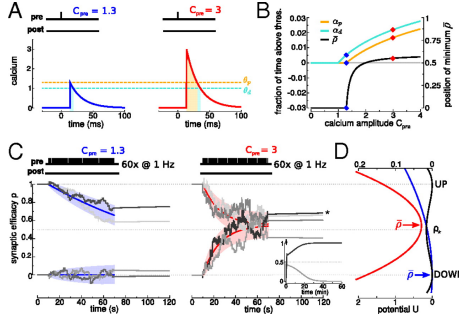


Figure 3.1: Behavior of the phenomenological model of Graupner & Brunel 2012. **A:** response of the postsynaptic calcium concentration to a presynaptic (left) and postsynaptic (right) bump. **B:** fraction of the time α that the calcium spends above depression and potentiation thresholds as a function of C_{pre} , when C_{post} is twice the value of C_{pre} , as would be approximately true at a typical synapse. **C:** Response of the phosphorylation variable ρ to the calcium bumps from A. The means are represented in bold, with a standard deviation on each side. A single trajectory is plotted in gray. On large time scales, the system falls back to one of the stable states based on its position relatively to their basin of attraction **D:** energy profiles for the two calcium histories of A. $\bar{\rho}$ is the average value that ρ reaches once the postsynaptic calcium concentration falls below both thresholds. **Courtesy of Graupner & Brunel 2012**

reached the synapse, the postsynaptic calcium level is assumed to instantly increase by parameter C_{pre} . When a postsynaptic spike arrives at the synapse through back action potential (bAP), the calcium concentration is assumed to rise by parameter C_{post} after a delay D . This delay represents the propagation of the bAP from the soma of the postsynaptic cell to the dendrite, which is assumed to be much slower than the propagation of a spike down the presynaptic axon added to the time of release, travel and capture of neurotransmitters from the presynaptic to the postsynaptic side. In the absence of any spike, the calcium concentration would decrease exponentially to zero, which approximates the basal concentration here. This calcium outflux represents the outpumping activity of membrane receptors in collaboration with transport proteins. It occurs at a time-scale τ_c

3.3 provides the response of the concentration of phosphorylated CaMKII sub-units to calcium. Here $\Theta(\cdot)$ is the Heaviside function. Let us go through each term of the right-hand side:

- First let's assume that only the first term (cubic term) of the RHS is there. We then have a rather direct equation for ρ , which has two stable states (0 and 1) and one unstable state $\rho^* \in]0, 1[$ of equilibrium. Based on where the initial phosphorylation level ρ_0 lies relatively to the basin of attractions of the stable states (who interface at $\rho = \rho^*$), the system will end either in a 'HIGH' ($\rho = 1$) activity state, or in a 'LOW' ($\rho = 0$) activity state, converging toward it with a speed $\frac{1}{\tau_{rho}}$. This term effectively provides the phosphorylation level the properties of stability that it demonstrates in the fine-grain model (Graupner and Brunel 2007) studied in the last chapter, modulo an affine rescaling.
- the third term $\gamma_d \rho \Theta(c(t) - \theta_d)$ represents the phenomenon of depression that occurs only when calcium is at values $\theta_d \leq c(t) \leq \theta_p$. When it does, activity level ρ is driven towards the 'LOW' activity state at speed $\frac{\gamma_d}{\tau_{rho}}$
- the second term $\gamma_p (1 - \rho) \Theta(c(t) - \theta_p)$ represents the phenomenon of potentiation that occurs only when calcium is above threshold value θ_p . This term only takes non-zero values when $c(t) \geq \theta_p$. When it does, the contributions from the third and a second term subtract. We chose to take $\gamma_d < \gamma_p$ so that when $c(t) \geq \theta_p$, we have net potentiation
- the fourth term $\sigma \sqrt{\Theta(c(t) - \theta_p) + \Theta(c(t) - \theta_d)} \eta(t)$ introduces noise into the behavior of ρ .

Noise is omnipresent in biological systems, neurons and synapses included. There are several sources of noise at different levels, including:

quantification noise coming from the fact that the PSD is a small region. For instance, only about 20 NMDA receptors live on the PSD, and about 80 CaMKII complexes are available there

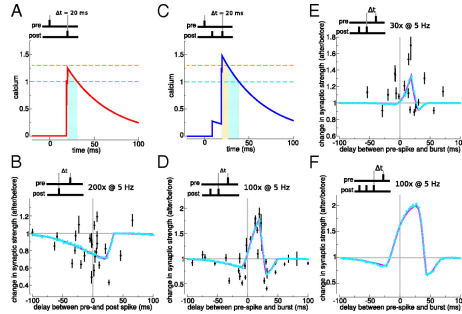


Figure 3.2: Fitting of the phenomenological model of Graupner & Brunel 2012 to experimental data from hippocampal slices (in vitro). Composition of each pairing (doublet, triplet or quadruplet), spike timing, number of pairings and frequency of the experimental protocols are provided above each STDP curve. **Courtesy of Graupner & Brunel 2012**

channel noise there are at least two places where channel noise is seen. On the axon, ion channels responsible for the emission and transmission of the action potential are inherently probabilistic, much like AMPA receptors on the membrane of the postsynaptic spine. Of course, the second place where we can find such noise is at the spines, both presynaptic (calcium influx from ion channels on the presynaptic side is responsible for the release of vesicles) and on the postsynaptic side

thermal noise

Here we model noise as a gaussian process. We show in appendix C that if we consider a fine-grain model like Graupner & Brunel 2007 or Michalski 2013, and if take into account quantification noise for each possible state of the CaMKII complex, the resulting noise on the concentration of active sub-units is itself gaussian.

This phenomenological model should be seen as a simplification of the fine grain model of Graupner and Brunel 2007 studied in the last chapter. We can clearly identify the two threshold θ_d (depression) and θ_p (potentiation), and we model the position of stable states and the dynamics of attraction at different calcium concentrations. The value of CaMKII activity at stable states is rescaled in the phenomenological model, to 0 for the 'LOW' state and 1 for the 'HIGH' state. In this regard, the phenomenological model should be seen as a tentative to mimic the dynamics of CaMKII activation through a simple, computationally actionable set of differential equations.

This model has several advantages. First of all, its parameters (among which $\tau_c, \tau_{rho}, \theta_d, \theta_p, \gamma_d, \gamma_p, D, C_{pre}, C_{post}$) all have a biophysical meaning and can be mapped to properties of either the fine-grain model from 2007 or of the synapse itself. The good incarnation of parameters has two consequences. Parameters are easy to interpret, they have intrinsic meaning. Second of all, tuning the parameters is made easier. Now, there is a need to contract this last statement: Graupner and Brunel did tune their parameters using their meaning, but there are a lot of them, and the system is nonlinear. To fit their model to experimental data, the authors did have to perform a parameter sweep within ansatz bounds, and then fine-tune parameters based on their respective meanings.

Second - and central - success of this model is that it successfully fits to experimental data from hippocampal slices (in vitro). For this purpose, the synaptic weight is assumed to be directly dependent on ρ through an affine mapping between w_{min} and w_{max} determined experimentally. Of course, the fact that the model was fit to in vitro data shows that further investigation to fit to in vivo data (which is far noisier, and sparse as it is harder to acquire) would be necessary to properly conclude on the model's capacity to reproduce early long-term plasticity. Figure 3.2 shows this fitting

Finally, this model is able to generate a large range of plasticity behavior, as far as STDP goes. Figure 3.3 shows how varying parameters C_{pre} and C_{post} can lead to a broad range of qualitatively different STDP curves, which represent the relative synaptic strength change $\frac{\Delta w}{w}$ as a function of the timing difference between the presynaptic and postsynaptic spikes Δt . Keep in mind that

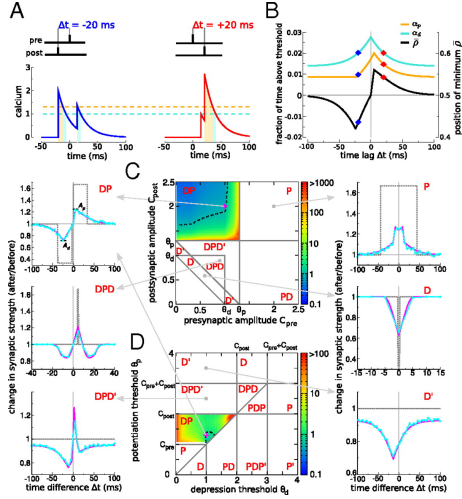


Figure 3.3: Qualitatively different STDP curves are obtained from the phenomenological model of Graupner & Brunel for 100 pairings at 10Hz by varying parameters C_{pre} and C_{post} . Different domains in the 2D place (C_{pre}, C_{post}) yield different kind of well known STDP curves, such as Hebbian STDP ($C_{post} > \theta_p, C_{pre} < \theta_p$). Anti-Hebbian plasticity can easily be obtained from Hebbian plasticity by exchanging values for C_{pre} and C_{post} . **Courtesy of Graupner & Brunel 2012**

those curves are obtained with 100 pairings at frequency 1Hz, and would typically evolve with both the number of spike pairings and with frequency.

3.1 Limitations of the base phenomenological model

Now is the time to take a step back and look at what we are trying to achieve here. Remember, what we want to do is have a calcium-based model of synaptic plasticity that we can implement into a network of, say, 10000 neurons. But wait... if this phenomenological model from Graupner & Brunel is so good at reproducing experimental data, is easily actionable and offers flexibility as to plasticity behavior, why did we bother to look into detailed molecular models of CaMKII and of synaptic plasticity? Why not use this model that provides phosphorylation ρ as a function of calcium history, and use this in our network?

The answer is that this model is not really actionable, at least not in general. This all has to do with noise. The molecular systems is intrinsically noisy. Let's assume that we start either in the 'HIGH' or 'LOW' phosphorylation level, and say that we have a given history of calcium coming in. Because the system is noisy, one cannot know for sure where the system stabilize once calcium concentration goes back to basal level. This is true as soon as calcium concentration spends time above the depression threshold.

In their paper from 2012, Graupner & Brunel have derived an analytical formula for the mean final activity level in the case of a group of independent synapses for which half start in the 'HIGH' state and the other half in the 'LOW' state, using the Fokker-Planck theory. For a general distribution of initial activity level, no formula is provided. That is a problem since in our neural network, we will need to update our network probabilistically based on an arbitrary initial condition.

When starting from an arbitrary initial condition, Graupner & Brunel use a Monte-Carlo method to estimate both the average response to a stimulus and the standard deviation. This has the following implication: each time we want to simulate the response in activity level of a single synapse to some calcium history, we do need to run K^2 simulations in order to get an estimate of the new synaptic weight such that the error is $\mathcal{O}(\frac{\sigma}{K})$ where σ itself has to be estimated. The accuracy/efficiency dilemma this introduce makes it impractical for an implementation in a network of several thousands neurons.

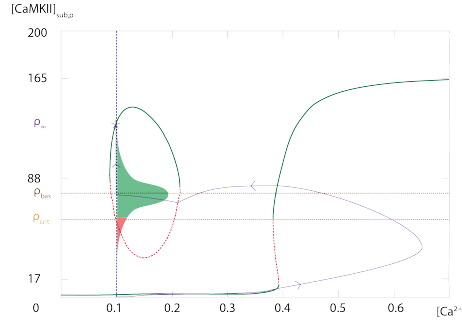


Figure 3.4: A trajectory of the system projected in the $([Ca^{2+}], S_p)$ plane. A history of calcium influx leads the CaMKII activity level to change. Activity reaches level ρ_{bas} at the moment the calcium concentration falls back to basal level. The position of ρ_{bas} relatively to ρ_{crit} along with our knowledge of the noise distribution allows us to know what the final average synaptic weight will be ($\rho_\infty = \rho_{max}$ in the present case). Once rescaled between 0 and 1, it is determined by the fraction of the noise distribution that lies below the dotted yellow line, which is the limits of the basins of attraction for the 'HIGH' (above) and 'LOW' (below) stable states at basal calcium concentration

3.2 Back to the detailed model: how can we bypass the Monte-Carlo trap?

Is there a way we could use our knowledge of the behavior of CaMKII at a fine-grain level to bypass sampling of the final synaptic weight? The good news is that we were able to show that the distribution of noise on the activity level is Gaussian under loose assumptions. Our idea is that we can leverage this information so that only one simulation needs to be run for an update to be known.

Figure 3.4 provides a graphic intuition. The idea is that all trajectories that lead the system to hit the line $[Ca^{2+}] = [Ca^{2+}]_{bas}$ above the dotted yellow line will eventually end up in the high activity state. Based on this, one can know the probability that a trajectory will end up in the high activity state by running a single simulation for the deterministic system (after removing the noise component in 3.3), and applying a transform that provides the integral of the noise distribution that is above the dotted yellow line:

$$\mathbb{E}(w_f) = 0 \int_{\rho=\rho_{crit}}^{\infty} p(\rho_{bas}) d\rho_{bas} \quad (3.4)$$

$$= \int_{x=\rho_{crit}-\rho_{bas}}^{\infty} q(x) dx \quad (3.5)$$

In 3.5 $p(\cdot)$ is the distribution of values for ρ_{bas} , and q is the distribution of the distribution of $\rho_{bas} - \bar{\rho}$ conditional to the deterministic system hitting line $[Ca^{2+}] = [Ca^{2+}]_{bas}$ at $\rho = \bar{\rho}$.

When assuming that the noise on CaMKII activity level is Gaussian, we can obtain an analytical formula on the value of the final synaptic weight:

$$w_f = \zeta(t_{bas}, \rho_{bas}) = erfc\left(\frac{\rho_{crit} - \rho_{bas}}{2\sigma^2(t_{bas})}\right) \quad (3.6)$$

In 3.6, t_{bas} is the time needed for the system to fall back to basal calcium concentration, and $\sigma(\cdot)$ is a function that provides the standard deviation of the Gaussian distribution of noise as a function of that duration:

$$\sigma(t) = \sigma_{eff} \sqrt{1 - \exp(-2n_{iter}\nu\tau_{eff})} \quad (3.7)$$

where

$$\begin{cases} \sigma_{eff} &= \sigma \sqrt{\frac{\alpha_{pot} + \alpha_{dep}}{G_{pot} + G_{dep}}} \\ \tau_{eff} &= (\alpha_{pot} + \alpha_{dep} > 0) \frac{\tau}{G_{pot} + G_{dep}} \\ \rho_{eq} &= \frac{G_{pot}}{G_{pot} + G_{dep}} \end{cases} \quad (3.8)$$

There are then two ways that we can use equation 3.6 to update the synaptic weight, each resulting in a synapse of a specific nature:

- we can choose to keep the synapse in our model bi-stable by setting the value of the synaptic weight w to 1 with a probability $\zeta(t_{bas}, \rho_{bas})$. This results in a probabilistic update and in a "digital" synapse with only two possible values for the synaptic weight
- alternatively, we could choose to allow the synapse in our model to take a continuum of values by taking directly $w = \zeta(t_{bas}, \rho_{bas})$. This is equivalent to studying the average weight of synaptic connections between a neuron A and a neuron B . In general in the hippocampus and the cortex, two neurons either share no synapse or share much more than one. Typically two connected neurons would share between one and three hundred synapses. When we go on and study, say, a fully-connected network of 10000 neurons, we can either model each of the 100 synapses between each pairs of neurons, resulting in 10^{10} edges, or we can model only an average synaptic connection between each pair of neurons, dividing the number of edges by 100. A large part of the process of late-LTP is deemed to be the genesis of new synapses between some neurons. One can therefore consider a 'mesoscopic' variable grouping the synaptic weights from the various synapses from A to B , using this variable as the effective strength of the connection from A to B (one may call it a connection weight). However, one must then keep in mind that an edge does not directly represent a single synapse.

We consider that both ways are interesting. They do lead to different networks, with different ways to analyze them. We started to investigate networks with edges representing averaged synaptic weights (second option), and plan to look at the first option in the future.

3.3 Continuously stable phenomenological model

In the end of this section we detail a phenomenological model of a group of synapses that we will then implement on a neural network. This model uses the update rule $w = \zeta(t_{bas}, \rho_{bas})$ introduced above.

Before we introduce our model, I will point out another limitation of model Graupner and Brunel 2012. One must keep in mind that in this model, synaptic plasticity is determined by the postsynaptic calcium level, which increases by a given amount C_{pre} or C_{post} in response to a spike (presynaptic or postsynaptic, respectively). This implies that following:

- Assume two neurons $A \rightarrow B$, such that neuron A fires at high frequency and neuron B does not fire at all. Our synapse may get so many presynaptic spikes that, during the course of firing, the presynaptic level would stabilize to a level way above the potentiation threshold. In effect, the synapse will potentiate
- The same goes with unilateral high-frequency postsynaptic neuron firing

While such behavior may be true of some neurons (who undergo only potentiation in response to unilateral high-frequency activity), this will typically not be the case for all neurons. For a significant part, a high-frequency presynaptic firing can lead to several phenomena of neural fatigue: synaptic vesicles can become too scarce for neurotransmitter transmission to keep up, and the postsynaptic membrane receptors can become overwhelmingly deactivated and unable to couple to high frequencies. It is therefore necessary to correct the model to include a phenomenon of synapse recuperation.

We therefore introduce recuperation variables x_{pre} and x_{post} to model the limited availability of synaptic resources at high-frequencies, and introduce the modified equation for postsynaptic calcium:

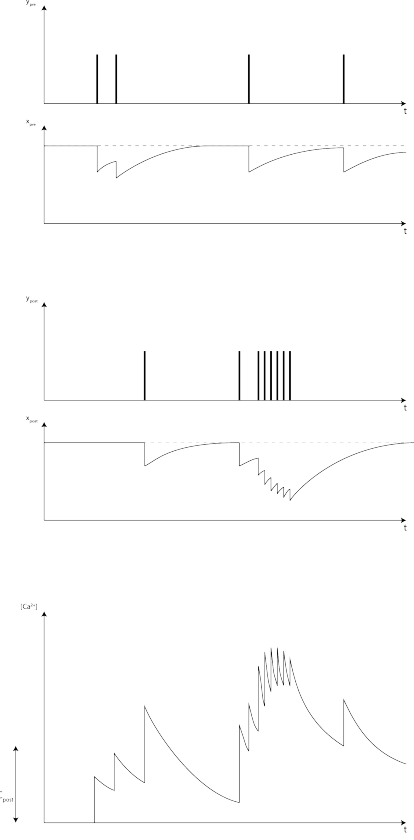


Figure 3.5: Response of recuperation variables and postsynaptic calcium concentration to an instance of presynaptic (y_{pre}) and postsynaptic (y_{post}) spikes history

$$\begin{cases} \tau_c \dot{c} = -c + C_{pre} \sum_{i \in I} x_{pre}(t) \delta(t - t_{pre}^{(i)}) + C_{post} \sum_{j \in J} x_{post}(t) \delta(t - t_{post}^{(j)}) \\ \tau_x \dot{x}_{pre} = (1 - x_{pre}) - r_{pre} x_{pre} \sum_{i \in I} \delta(t - t_{pre}^{(i)}) \\ \tau_x \dot{x}_{post} = (1 - x_{post}) - r_{post} x_{post} \sum_{j \in J} \delta(t - t_{post}^{(j)}) \end{cases} \quad (3.9)$$

x_{pre} and x_{post} have the effect of having the unit calcium influx decrease with spike frequency according to:

$$x_\infty = \frac{\exp \frac{1}{\tau_x \nu} - 1}{\exp \tau_x \nu + 1}$$

where ν is the spike frequency. Each of these recuperation variables is parameterized by a recuperation time constant τ_x (taken to be the same on both side for simplicity) and a fatigue rate r . On the presynaptic side, this last parameter can be interpreted as the fraction of membrane receptors that become deactivated in response to a single presynaptic spike. On the postsynaptic spike, it can be interpreted as the fraction of dendritic ion channels that deactivate per bAP. Figure

All in all, our phenomenological model can be described by five ODEs per connection $A \Rightarrow B$:

$$\begin{cases} \tau_c \dot{c} = -c + C_{pre} \sum_{i \in I} x_{pre}(t) \delta(t - t_{pre}^{(i)}) + C_{post} \sum_{j \in J} x_{post}(t) \delta(t - t_{post}^{(j)}) \\ \tau_x \dot{x}_{pre} = (1 - x_{pre}) - r_{pre} x_{pre} \sum_{i \in I} \delta(t - t_{pre}^{(i)}) \\ \tau_x \dot{x}_{post} = (1 - x_{post}) - r_{post} x_{post} \sum_{j \in J} \delta(t - t_{post}^{(j)}) \\ \tau_\rho \dot{\rho} = \rho(1 - \rho)(\rho^* - \rho) + \gamma_p(1 - \rho)\Theta(c(t) - \theta_p) - \gamma_d \rho \Theta(c(t) - \theta_d) \\ \tau_w \dot{w} = w - \frac{1}{2} \operatorname{erfc}\left(\frac{S_{attr} - \rho}{2\sigma(t_{stop} - t_0)^2}\right) \end{cases}$$

3.4 Analysis framework and results for the phenomenological model

Our model needs to be characterized on several fronts. We will aim to answer the following questions:

Fit to experimental data including:

- Can the model reproduce experimental data for STDP curve? Can we still obtain as wide a range of plasticity curves by changing parameters?
- Can we reproduce the experimental data on the dependence of plasticity on frequency by tuning parameters r_{pre} , r_{post} and τ_x ?

Analytical simplicity Do we have any analytical formula for the response of our model to spike pairs? For response to random presynaptic and postsynaptic following some given laws?

Computational simplicity How fast is the model for simulating the evolution of synaptic weight?

Answering those questions will help us assess our phenomenological model. Not only do we want to understand how the model respond to a given stimulation protocol, we also want to understand how each group of synapse will behave locally once it is plugged into the network, as a function of the statistics of the presynaptic and postsynaptic neurons.

To answer those questions, I developed a framework in Matlab that simulates the evolution of synaptic weight as a function of any given stimulation protocol, and allows for the following analysis:

- single protocol response
- STDP curve
- spike-timing vs frequency reponse
- spike-timing vs number of pairing response
- fit to experimental data in the spike-timing cd number of frequency plane
- response to presynaptic and postsynaptic Poisson processes, with and without correlation

All results are computer analytically, meaning that we do not need to integrate the ODEs over fixed time steps. Rather, we split our protocol into bits during which no spike arrive at the synapse, and we update the system based on the length of those bits and on the spike events in between them. We integrate the ODEs with analytical formulas on those time periods. Integrating the equations governing the synapses in such a manner allows for a fast simulation of the evolution of the network.

The behavior of our system in response to an arbitrary protocol is provided in figure (BIND WITH ILLUSTRATOR).

3.4.1 Richness of the model

The first thing to notice is that our model is a generalization of the model by Graupner & Brunel (2012) as far as phosphorylation goes: one can chose to take saturation rates r_{pre} and r_{post} equal to zero and would end up with precisely the same behavior for ρ . However, one must also note that we are interested in the response of the system for different frequencies and number of stimulation pairs, for instance. However, we intuitively see that the response of the system as a function the protocol will be altered by this saturation in an unpredictable way:

- on one hand, the higher the frequency, the closer to 0 the regeneration variables x_{pre} and x_{post} will be after transient period, leading to lower levels of calciums let into the cell
- on the other hand, for high enough frequencies, the saturation phenomenon can be over-weighted by the volume of spikes, leading to higher levels of calcium let into the cell

Our simulations do show that the effect of damping is nonlinear and translate this competition between saturation and volume effects.

A first question that we face is thus:

Look at the response of the system for a stimulation protocol for n pairs. Looking at STDP curves ($\frac{\Delta w}{w}$ vs dt) generated at different stimulation frequencies, *can we reproduce behavior recorded experimentally? Can our model capture the broad range of behaviors observed within the brain in terms of (STDP,frequency) curves?*

We started by fitting our model to experimental data from inhibitory synapses in hippocampal slices by Laurent Venance, our collaborator at Collège de France and expert in electrophysiology. The plasticity that Laurent typically observes in this region of the brain for mice is anti-Hebbian. To obtain the data, the Venance Lab first preconditions the brain slices with ionic and proteic baths and given physical conditions so as to initialize the cells in preferred states in terms of potentials, ionic and proteic composition so as to reproduce in vivo concentrations as well as possible. When looking at in vivo cells, such a process is of course unnecessary, but heavier experimental processes are required so as to acquire quality data.

In appendix A, we provide different sets of parameters that allow to obtain qualitatively different behaviors in terms of STDP at 1Hz. One can also look at the evolution of plasticity with increasing frequency, and see that potentiation becomes increasingly likely whatever the time delay, for all provided sets of parameters.

3.4.2 Experimental protocol

The stimulation protocol is defined by excitatory currents applied to axonal or dendritic regions using patch clamp techniques. Note that in general a current injection stimulates tens to hundreds of axonal or dendritic branches at the same time, generally belonging to different neurons. This is due to mere technical considerations as to what spatial specificity can be achieved in the stimulation protocol. When we can make sure that both the presynaptic and postsynaptic neurons of a given synapse can be targeted at will and independently, the stimulation protocol applied is the one described previously: the presynaptic neuron is excited for n repetitions at frequency f Hz, and the postsynaptic is stimulated in the same way with a temporal shift dt which can be positive (PRE CELL then POST CELL) or negative (POST CELL then PRE CELL).

3.4.3 Defining STDP in our model

In our model one must take note that the synaptic weight obtained after a stimulation protocol is submitted depends not only on the protocol, but also on the initial value of the activity level. To characterize the behavior of our model in terms of spike-timing dependency, we look at the following:

$$\frac{\Delta w}{w}(\Delta t) = \int_{\rho_0=0}^{\rho_{max}} \frac{\zeta(\rho_f(\rho_0, \Delta t)) - \zeta(\rho_0)}{\zeta(\rho_0)} \quad (3.10)$$

where, in 3.10, Δt is the delay from presynaptic postsynaptic spike within the protocol.

3.4.4 Fitting STDP behavior of hippocampal slices

We looked for a set of parameters that would result in the system reproducing the behavior of synapses of in vitro pyramidal cells of the CA3 pathway (neurons in a specific area of the hippocampus, which is the most studied area for plasticity). We fit our model to the data so that not only the curve $\frac{\Delta w}{w} = f(dt)$ would fit the experimental data at a given frequency ν , but more so that the surface $\frac{\Delta w}{w} = g(\nu, dt)$ would properly fit the experimental data across the range of protocol frequencies that was tested by the Venance lab. Figures ?? to ?? show one of our fit.

Figure 3.8 provides the fit of our surface $\frac{\Delta w}{w} = g(\nu, dt)$ to the experimental data (data for each fixed frequency is represented by a ribbon. Comparing the position of the ribbon to that of the curve provides a data fit at a fixed frequency similar to figures ?? to ??). For any set of biologically plausible parameters, the model will exhibit an increase in relative change of plasticity with frequency: the higher the stimulation frequency, the more the synapse is likely to potentiate regardless of how presynaptic and postsynaptic spikes are timed relatively to one another, and the less it is likely to depress. The potentiation threshold for calcium explains this behavior. Similarly,

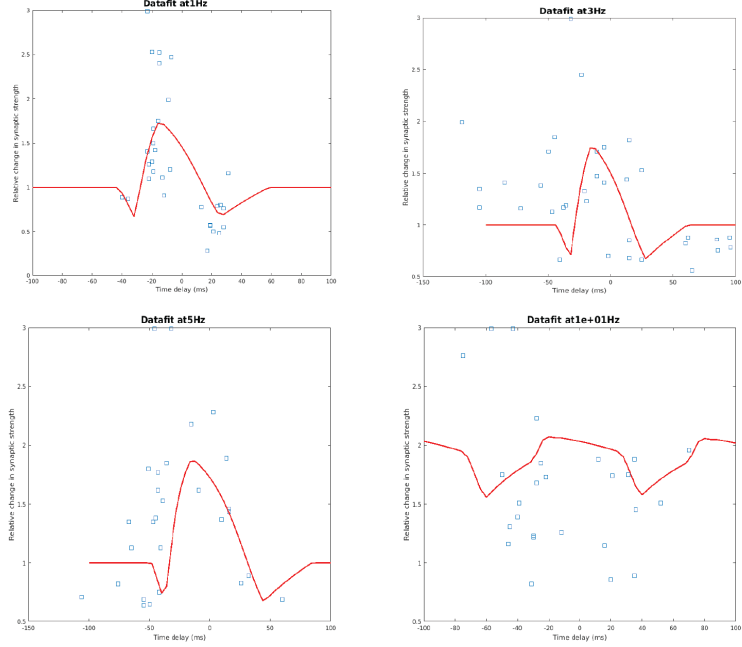


Figure 3.6: Fitting our model to experimental data from pyramidal cells in the hippocampus of mice (in vitro). Data was collected by Venance et al, for different experimental protocols, consisting of exciting the presynaptic and postsynaptic cells for 100 pairings at a given frequency **Top left:** 1Hz **Top right:** 3Hz **Bottom left:** 5Hz **Bottom right:** 10Hz

there are parameter values for which we see an intermediate range of frequencies, at which the synapse is more likely to depress. This is especially likely to happen when the potentiation threshold is much higher than the depression threshold, and that the calcium bumps cause by single stimuli are lower than the depression threshold. This phenomenon is of course inherent to the presence of thresholds in the model.

3.4.5 Response of the model to Poisson firing

The original motivation of our model is to have a rule that can work on a network of spiking neurons. In such a network, neurons $A \rightarrow B$ can display a wide range of behaviors, from synchronous firing at fairly constant frequency to asynchronous firing at irregular times. In the case of asynchronous irregular firing, it can be useful to consider in first instance that two arbitrary neurons behave independently at a given time. This approximation, though sometimes quite coarse, we can sometime derive some analytical formula about the system in this case.

In general, it is important to know how our model of plasticity responds to random activities of a presynaptic and postsynaptic neurons, when those activities are uncorrelated. We can also look at correlated spiking activities at least for some cases of cross-correlation functions. Because we are dealing with spiking events, modeling spike trains as point processes provides a good framework for analysis. Here we will consider that spike trains follow inhomogeneous Poisson processes. Those are point processes of the form:

$$y(t) = \sum_{i \in I} \delta(t - t_i)$$

where t_i are spike times, such that the interspike interval follows an exponential distribution of intensity $\nu(t)$. The probability density function for the interspike interval would be:

$$p_t(s) = \nu_t \exp(-\nu_t s) \mathbf{1}_{s \geq 0}$$

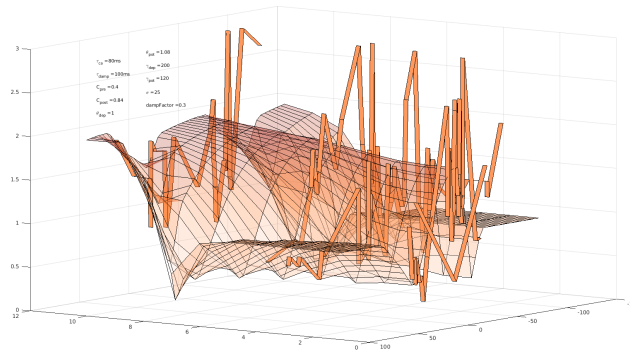


Figure 3.7: Our model fit to the data from the Venance lab. The surface is produced by our model. Each ribbon represents the experimental plasticity curve at a given frequency. The parameters of the model are plotted on the top left

We can analyze the response of our model of synaptic plasticity to neurons with Poisson spike trains. Even though some elements in our model can be derived analytically (in Gilbert and H.O 1960 Gilbert provides the elements to derive a formula for the distribution of Calcium in response to independent Poisson spiking events). However, a full analysis is not possible for our model past calcium concentrations and recuperation variables. Therefore we used simulation to investigate the response of our model.

Figure ?? provides the response of the model in terms of relative change in synaptic strength as a function of the frequencies of the Poisson processes for both the presynaptic and the postsynaptic rates. The value of the parameters to obtain this curve were chosen so that in the region of the (ν_{pre}, ν_{post}) space where the network would typically work in, there would be both potentiation and depression. This ensures that the weights of the network do not follow a trivial behavior (for instance, all synapses depress to the minimum value, or all potentiate to the maximum value). We will dive in more details about the role of presynaptic and postsynaptic spike rates when we look at the behavior of our model within a network of spiking neurons. As of now one can note several properties of this response:

- the large asymmetry in the role of presynaptic and postsynaptic rate, which to a large extent depends on the value of the parameters
- in general, the higher the frequency of the system, the more the system "responds", in the sense that both depression and potentiation tend to become more intense when frequency increase

How can we choose a set of parameters for our model of synapse, so that when we build a network of spiking neurons with such synapses, the network does not behave in a trivial way (full potentiation or full depression)? Our idea is that parameters should be chose so that in the range of firing frequencies that are most typical of the network, we find both potentiation and depression in Fig ??, in a balanced fashion. However, the typical frequencies of the network depend themselves on the synaptic weights. This chicken and egg problem is one of our future research directions.

Finally, understanding the behavior of a synapse when presynaptic and postsynaptic firing are correlated is important, since such correlations will exist in the network. We are currently working on testing the response of synapses to correlated Poisson processes, using the methods of simulation by Brette (Brette 2009). Overall, we hope to develop a theoretical framework on the lines of Ocker, Litwin-Kumar, and Doiron 2015 that would allow us to better understand the behavior of a network of spiking neurons with plastic synapses.

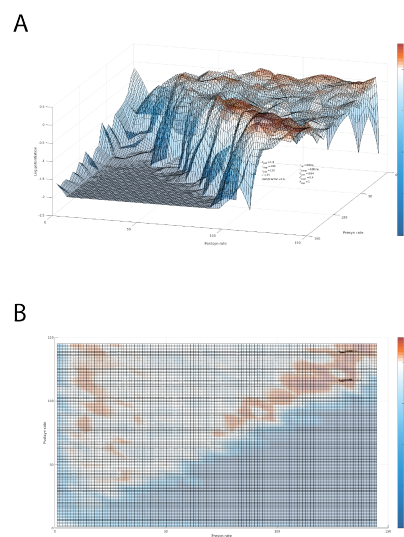


Figure 3.8: Response of our model of plasticity when presynaptic and postsynaptic neurons spiking events follow independent Poisson processes. The z-axis represents the logarithm of the relative change in synaptic weight. **Top:** The x and y axes represent the frequencies of the presynaptic and postsynaptic spiking events, respectively. The values of parameters are indicated on the bottom right and were chosen so that in the typical regime of frequencies in our network, we would observe both depression and potentiation, so that the evolution of synaptic weights in the network would be nontrivial. **Bottom:** Colormap of the response

Chapter 4

Network-wide properties of the calcium-based model

In the last chapter of this report, I provide some results and simulations for a specific architecture of spiking networks.

4.1 Network architecture and biological motivation

Our main interest in this last part of our investigation is to understand how our plasticity rule would modulate a network of neurons, and whether this rule (that reproduces STDP curves) could indeed be sufficient to train the network to remember time sequences such as audio recordings or movies.

There is a wide corpus of literature on networks of spiking neurons. We studied a popular model of sparsely-connected neural networks, studied by Amit and Brunel (Amit and Brunel 1997, Brunel 2000). The network is said to be **balanced**, because it contains both excitatory cell and inhibitory cell; their relative activity tightly controls global behavior. Brunel has established maps of global behavior of the network that depend on two parameters: the strength of inhibitory synapses relatively to excitatory synapses, and the strength of an unstructured input signal that is given to all synapses. We used this analysis has a starting point to look at the evolution of global activity when we allow the synapses in our network to evolve with time.

The network is made of $N = N_E + N_I$ neurons, N_E of which are excitatory (they positively contribute to the depolarization of the neurons they are directly connected to) and N_I of which are inhibitory. It is sparsely connected: each neuron receives connections for a fraction ϵ of all neurons: $C_E = \epsilon N_E$ from excitatory neurons, $C_I = \epsilon N_I$ from inhibitory neurons.

In the static model of Brunel 2000, denote $E \rightarrow I$ a connection from an excitatory cell to an inhibitory cell, $E \rightarrow E$ a connection from excitatory to excitatory, etc.

- the synaptic weight for $E \rightarrow \cdot$ would be w
- the synaptic weight for $I \rightarrow \cdot$ would be $-gw$

Additionally, each cell receives an input from outside of the network. In the static model those outputs are considered to be random, following independent Poisson processes with frequencies ν_{ext} .

Brunel found that the systems has a global behavior that depends on two parameters: the exterior input frequency ν_{ext} relative to a threshold frequency ν_{thr} , and the strength of inhibitory synapses relatively to excitatory synapses, g . The results can be plotted in the plane $(\frac{\nu_{ext}}{\nu_{thr}}, g)$ as seen in Fig 4.2. There are four regimes: Synchronous Regular (SR), fast Synchronous Irregular (SI fast), slow Synchronous Irregular (SI slow) and Asynchronous Irregular (AI). Fig 4.3 provides examples of firing activity for each regime.

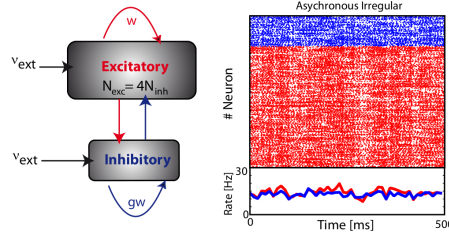


Figure 4.1: **Left:** Architecture for the network of Brunel 2000 that we use a starting point. Connection strength between neurons depend on the nature of the presynaptic neuron. Input currents from exterior cells are applied regardless of the neuron, as independent Poisson processes of frequencies ν_{ext} . In this example, there are four times as many excitatory cells as there are inhibitory cells. **Right:** A raster plot of the spike times for a balanced network of 250 neurons. Courtesy of Pierre Yger

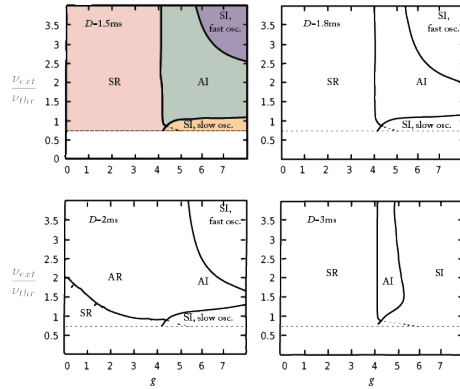


Figure 4.2: Regime of firing of neurons in the network as a function of $\frac{\nu_{ext}}{\nu_{thr}}$ and g . Four distinct regimes of activity can be found, with domains varying in shapes when the delay of transmission of a spike D is varied. Courtesy of Nicolas Brunel

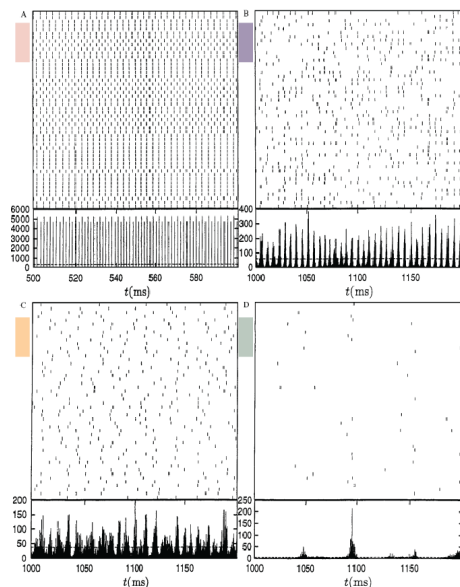


Figure 4.3: Four rasterplots each corresponding to a regime. Regimes are mapped to raster plots using the color code of Fig 4.2

4.2 Implementation of calcium-based plasticity rule in the network

The first question to answer when implementing our plasticity rule onto the network from Brunel 2000 is: what becomes the spontaneous behavior of the network? In particular:

- Does the network stabilizes? If so, how do the stable states depend on the parameters of the synapses?
- What is the influence of the exterior input on the spontaneous behavior? We can think of both the influence of ν_{ext} when all neurons take as input independent Poisson spikes at a same frequency, or the distribution of input frequencies when the input signal is "structured"
- How do synaptic weights evolve, and what is their distribution in a stable configuration?
- Does the network spontaneously stabilizes in a global firing regime? Does it alters between regimes in a timely manner? Is the behavior chaotic?

We could choose among many configurations of initial synaptic weights. We started to investigate the evolution of the network with two different initializations:

- when it is initialized as in Brunel 2000, with inhibitory synapses scaling excitatory synapses to a ratio g in strength
- when synaptic weights are initialized randomly, with inhibitory synapses expected to scale by g relative to excitatory synapses

Using the plasticity parameters provided in appendix A, we developed tools to vizualize the spontaneous activity of the network (here spontaneous means that the exterior input is not structured, ie we are not trying to teach the network to reproduce a pattern by applying specific, structured patterns of input signals to it).

We provide an example of network behavior on Fig4.4.

We are currently in the phase of asserting the role of parameters in the behavior of the network, as well as the role of initial conditions and the statistics of the input noise. Our first objective is to understand how to choose parameters of the synapse model so as to have a non-trivial activity for the network, like that of Fig4.4 (the distribution of synaptic weights converge to a distribution that is not fully concentrated at zero. Better, it is multimodal with a principal mode around a value that seem to depend on parameter values).

4.3 Future research directions

STDP behavior as a function of number of pairings A well-known property of STDP plasticity in response to pair of spikes is variation of the behavior with the number of pairs (see for instance Vignoud, Venance, and Touboul 2018) find that when increasing the number of spike pairings, different responses can occur. Typically, for a Hebbian kind of STDP, there can be a range of frequencies at which the typical response of the system "softens", so that the synapse is less depressed for negative delays and less potentiated for positive delays (see REFERENCE HERE). This property of STDP was not tested yet on our model, and is part of our next steps.

Theoretical framework to understand network of spiking neurons with plastic synapses
Ideally, we would like to show a relationship between the frequency of excitation of the network ν_{ext} and the global behavior of the system in large times. Ocker, Doiron et al (Ocker, Litwin-Kumar, and Doiron 2015) built a framework that works with additive STDP rules. They found a relationship between the integral of the STDP rule (ie, is it biased towards potentiation, biased toward depression or balanced?) and the characterization of stable states for the first momenta of the synaptic weights. Their analysis also depends on the cross-correlations between the presynaptic and postsynaptic spikes. We would like to conduct a similar analysis for calcium-based, ODE-based synaptic plasticity rules.

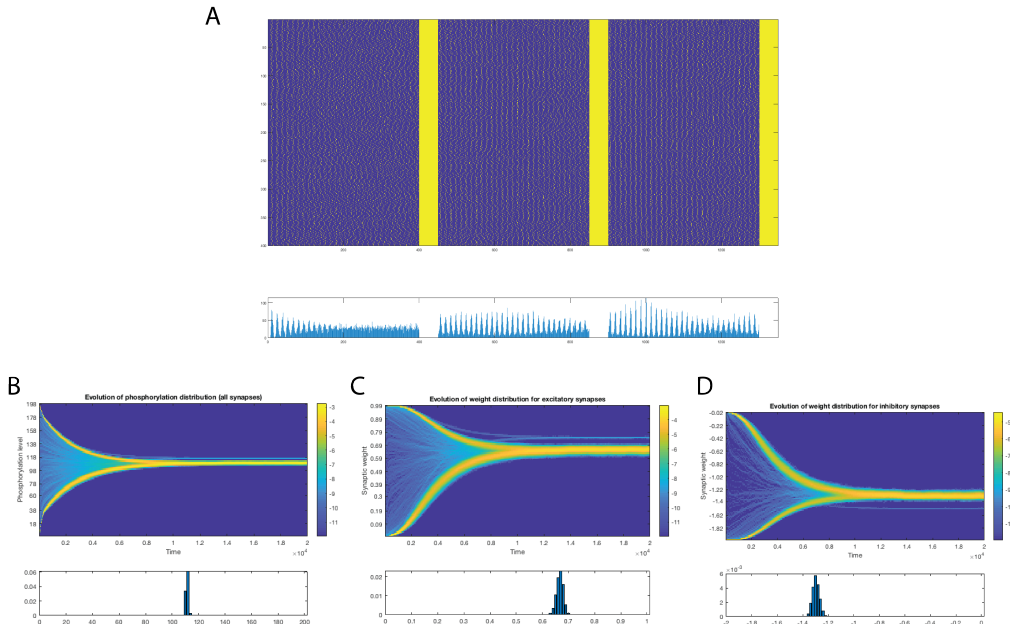


Figure 4.4: Spontaneous behavior of the network of 400 LIF neurons from Brunel 2000 when synapses follow our model, having been initialized randomly. Simulating 20s of activity took 3min of computation with a mid-range laptop. **A:** raster plots for the duration of the simulation. On the bottom is the total activity per time step. Yellow vertical bars represent discontinuities in time, as we are interested in the evolution of the system at large times. The initial synchrony is artificial, purely due to the way the network is initialized. The system then quickly falls into an asynchronous state with only small variations in firing frequencies. Over large times, the system returns to a state of synchrony. There seems to be a periodic behavior of slight desynchronization and resynchronization, but further study is required to confirm that this phenomenon is consistently caused by parameters and not by some sets of initial conditions. **B:** Evolution of the logarithm of the probability distribution of the phosphorylation level. Like the synaptic weights, phosphorylation levels across the network are initialized randomly, but in large time converge to a tight distribution. **C:** Evolution of the logarithm of the distribution of synaptic weights for excitatory synapses. **D:** Evolution of the logarithm of the distribution of synaptic weights for inhibitory synapses. Notice that the distributions in **B**, **C**, **D** are not unimodal. Even though the second mode is much smaller, it consistently exists in large times for random initializations

Testing performance of the network to learn time sequences, proceeding along the lines of Nicola and Clopath 2017. In this article, Nicola and Clopath use a supervised learning algorithm for spiking networks called FORCE (Sussillo and Abbott 2009). The architecture of the network is similar, and they successfully teach the network to autonomously reproduce dynamical systems (for instance a Lorentz attractor), time sequences (the first few notes of Ode to Joy, the singing of a zebra finch). Whether or not an unsupervised learning rule based on calcium, and that can reproduce spike-timing dependency, is able to learn such time-sequences is a major question. We would like to tackle this question using our rule of synaptic plasticity.

4.4 Conclusion

During this internship, we successfully developed a model of synaptic plasticity that simultaneously answers to multiple criteria: it can fit experimental data from a wide range of neurons in different areas of the brain. It has few parameters, which all have a biophysical meaning. The model is light-weight and consists of five ordinary differential equations per synapse. Most importantly, we rely on a deterministic system to have a single instance of equations to integrate in order to simulate a synapse. Through the analysis of fine-grain, molecular models of synaptic plasticity, we have derived a rule to obtain the synaptic strength as a function of a molecular activation variable. The mapping from the latter to the former depends on the distribution of noise for the activation variable, which we have shown can be considered Gaussian.

Having developed a light-weight rule for synaptic plasticity, we have shown that our model offers the same breadth of behavior than the phenomenological model developed by Graupner and Brunel (Graupner and Brunel 2012). It also takes into account phenomena of saturation of the membrane receptors; this has some interesting consequences on the response of the model in frequency. More importantly, this allows us to control the impact of unilateral firing on synaptic plasticity.

We can successfully generate tens of seconds of activity for a network of 2000 LIF neurons in approximately 10 minutes on a high-end laptop, and seconds for a 500 LIF neurons network in less than a minute. This allows us to study the interaction of network architecture and synaptic plasticity very easily. In turn, we will use these simulations to both help us develop a theoretical framework, and for teaching time-sequences to the network.

We limited our study to a specific context, as it offered better opportunities. In particular, synapses of the Schaffer collater in the hippocampus have been widely studied, and many rules of synaptic plasticity were developed through confrontation to experimental data from this area. However, our model of synaptic plasticity is general, as variation of the postsynaptic calcium concentration has been shown to be both necessary and sufficient for the induction of plasticity for a wide range of synapses in several brain areas. In particular, we believe our model applies well for cortico-striatal and thalamo-striatal synapses.

We also focused solely on homosynaptic plasticity, meaning the plasticity that involved a single synapse without considering the interaction between multiple synapses. Finally, let us recall here that our aim has been to model the induction of plasticity with a retention of information on the order of tens of minutes maximum. There are other mechanisms, some triggered by the chemical pathways that we have studied, that are known to "take over" plasticity, in the sense that the information that is stored chemically at first can be translated into structural changes at the synapse of local expression or repression of some genes in the soma (epigenetics). We did not have any ambition to model such phenomena.

Our efforts need to be carried on in the coming months. We hope to be able to show that calcium-based plasticity can effectively learn sequences in networks, which we believe has never been done before. We also hope to be able to come back to our study of fine-grain models, to reach conclusion regarding the stability of CaMKII phosphorylation in the general case presented at the end of chapter 1.

4.5 Our code

The frameworks we used to analyze phenomenological models of plasticity (both at the level of one synapse and within the network from Brunel 2000) is available at:

https://github.com/slebastard/STDP_Pheno_CalciumSynapticPlasticity

The Git will be updated regularly until the project ends, and I plan on adding some improvements, such as a GUI for user-friendly parametrization of the synapse, network and simulations. The documentation will also be updated.

The code that we used to study fine-grain models of plasticity is available at:

https://github.com/slebastard/STDP_Detailed_CaMKIIPathway

I do plan to improve this Git and make it more approachable, but it is not usable by anyone else at the moment.

Bibliography

- [AB97] DJ Amit and Nicolas Brunel. “Model of global spontaneous activity and local structured activity during delay periods in the cerebral cortex”. In: *Cerebral Cortex* (Apr. 1997). URL: <https://www.ncbi.nlm.nih.gov/pubmed/9143444>.
- [Bay+01] K. -Ulrich Bayer et al. “Interaction with the NMDA receptor locks CaMKII in an active conformation”. In: *Nature* 411 (June 2001), 801 EP -. URL: <http://dx.doi.org/10.1038/35081080>.
- [Bli+95] RD Blitzer et al. “Postsynaptic cAMP pathway gates early LTP in hippocampal CA1 region”. In: *Neuron* (Dec. 1995). URL: <https://www.ncbi.nlm.nih.gov/pubmed/8845163>.
- [BN03] David S. Bredt and Roger A. Nicoll. “AMPA Receptor Trafficking at Excitatory Synapses”. In: *Neuron* 40.2 (Oct. 2003), pp. 361–379. ISSN: 0896-6273. DOI: [10.1016/S0896-6273\(03\)00640-8](https://doi.org/10.1016/S0896-6273(03)00640-8). URL: [https://doi.org/10.1016/S0896-6273\(03\)00640-8](https://doi.org/10.1016/S0896-6273(03)00640-8).
- [BP98] Guo-qiang Bi and Mu-ming Poo. “Synaptic Modifications in Cultured Hippocampal Neurons: Dependence on Spike Timing, Synaptic Strength, and Postsynaptic Cell Type”. In: *Journal of Neuroscience* 18.24 (1998), pp. 10464–10472. ISSN: 0270-6474. DOI: [10.1523/JNEUROSCI.18-24-10464.1998](https://doi.org/10.1523/JNEUROSCI.18-24-10464.1998). eprint: <http://www.jneurosci.org/content/18/24/10464.full.pdf>. URL: <http://www.jneurosci.org/content/18/24/10464>.
- [Bre09] Romain Brette. “Generation of Correlated Spike Trains”. In: *Neural Computation* 21.1 (2009), pp. 188–215. DOI: [10.1162/neco.2009.12-07-657](https://doi.org/10.1162/neco.2009.12-07-657). eprint: <https://doi.org/10.1162/neco.2009.12-07-657>. URL: <https://doi.org/10.1162/neco.2009.12-07-657>.
- [Bru00] Nicolas Brunel. “Dynamics of Sparsely Connected Networks of Excitatory and Inhibitory Spiking Neurons”. In: *Journal of Computational Neuroscience* 8.3 (May 2000), pp. 183–208. ISSN: 1573-6873. DOI: [10.1023/A:1008925309027](https://doi.org/10.1023/A:1008925309027). URL: <https://doi.org/10.1023/A:1008925309027>.
- [CIW04] Graham L. Collingridge, John T. R. Isaac, and Yu Tian Wang. “Receptor trafficking and synaptic plasticity”. In: *Nature Reviews Neuroscience* 5 (Dec. 2004). Review Article, 952 EP -. URL: <http://dx.doi.org/10.1038/nrn1556>.
- [Con+15] Audrey Constals et al. “Glutamate-Induced AMPA Receptor Desensitization Increases Their Mobility and Modulates Short-Term Plasticity through Unbinding from Stargazin”. In: *Neuron* 85.4 (2015), pp. 787–803. ISSN: 0896-6273. DOI: <https://doi.org/10.1016/j.neuron.2015.01.012>. URL: <http://www.sciencedirect.com/science/article/pii/S0896627315000380>.
- [Cui+15] Yihui Cui et al. “Endocannabinoids mediate bidirectional striatal spike-timing-dependent plasticity”. In: *J Physiol* 593.Pt 13 (July 2015). 25873197[pmid], pp. 2833–2849. ISSN: 0022-3751. DOI: [10.1113/JP270324](https://doi.org/10.1113/JP270324). URL: <http://www.ncbi.nlm.nih.gov/pmc/articles/PMC4506184/>.
- [DE12] Feldman DE. “The spike timing dependence of plasticity”. In: *Neuron* 4.75 (2012). doi:10.1016/j.neuron.2012.08.001, pp. 556–571.
- [Erm16] Bard Ermentrout. *XPPAut 8.0*. <http://www.math.pitt.edu/~bard/xpp/xpp.html>. 2000–2016.

- [Faa+11] Guido C Faas et al. “Calmodulin as a direct detector of Ca²⁺ signals”. In: *Nature Neuroscience* 14 (Jan. 2011), pp. 301–. URL: <http://dx.doi.org/10.1038/nn.2746>.
- [GB07] Michael Graupner and Nicolas Brunel. “STDP in a Bistable Synapse Model Based on CaMKII and Associated Signaling Pathways”. In: *PLOS Computational Biology* 3.11 (Nov. 2007), e221–. DOI: [10.1371/journal.pcbi.0030221](https://doi.org/10.1371/journal.pcbi.0030221). URL: <https://doi.org/10.1371/journal.pcbi.0030221>.
- [GB10] Michael Graupner and Nicolas Brunel. “Mechanisms of Induction and Maintenance of Spike-Timing Dependent Plasticity in Biophysical Synapse Models”. In: *Frontiers in Computational Neuroscience* 4 (Aug. 2010), pp. 136–. ISSN: 1662-5188. URL: <http://www.ncbi.nlm.nih.gov/pmc/articles/PMC2953414/>.
- [GB12] Michael Graupner and Nicolas Brunel. “Calcium-based plasticity model explains sensitivity of synaptic changes to spike pattern, rate, and dendritic location”. In: *Proceedings of the National Academy of Sciences of the United States of America* 109.10 (Feb. 2012), pp. 3991–3996. ISSN: 1091-6490. URL: <http://www.ncbi.nlm.nih.gov/pmc/articles/PMC3309784/>.
- [GCC98] F Gardoni, A Caputi, and M Cimino. “Calcium/calmodulin-dependent protein kinase II is associated with NR2A/B subunits of NMDA receptor in postsynaptic densities”. In: *Journal of Neurochemistry* (Oct. 1998), pp. 1733–1741. URL: <https://www.ncbi.nlm.nih.gov/pubmed/9751209>.
- [Ger+96] Wulfram Gerstner et al. “A neuronal learning rule for sub-millisecond temporal coding”. In: *Nature* 383 (Sept. 1996), 76 EP -. URL: <http://dx.doi.org/10.1038/383076a0>.
- [GH60] E.N Gilbert and Pollak H.O. “Amplitude Distribution of Shot Noise”. In: *Bell System Technical Journal* (1960). URL: <https://onlinelibrary.wiley.com/doi/abs/10.1002/j.1538-7305.1960.tb01603.x>.
- [Heb88] Donald O. Hebb. *Neurocomputing: Foundations of Research*. Ed. by James A. Anderson and Edward Rosenfeld. Cambridge, MA, USA: MIT Press, 1988. Chap. The Organization of Behavior, pp. 43–54. ISBN: 0-262-01097-6. URL: <http://dl.acm.org/citation.cfm?id=65669.104380>.
- [Hel14] Johannes W. Hell. “CaMKII: Claiming Center Stage in Postsynaptic Function and Organization”. In: *Neuron* 81.2 (Jan. 2014). 24462093[pmid], pp. 249–265. ISSN: 0896-6273. DOI: [10.1016/j.neuron.2013.12.024](https://doi.org/10.1016/j.neuron.2013.12.024). URL: <http://www.ncbi.nlm.nih.gov/pmc/articles/PMC4570830/>.
- [HGB14] David Higgins, Michael Graupner, and Nicolas Brunel. “Memory Maintenance in Synapses with Calcium-Based Plasticity in the Presence of Background Activity”. In: *PLOS Computational Biology* 10.10 (Oct. 2014), pp. 1–16. DOI: [10.1371/journal.pcbi.1003834](https://doi.org/10.1371/journal.pcbi.1003834). URL: <https://doi.org/10.1371/journal.pcbi.1003834>.
- [HKF02] Richard H. R. Hahnloser, Alexay A. Kozhevnikov, and Michale S. Fee. “An ultra-sparse code underlies the generation of neural sequences in a songbird”. In: *Nature* 419 (Sept. 2002), 65 EP -. URL: <http://dx.doi.org/10.1038/nature00974>.
- [HKS15] Y. He, D. Kulasiri, and S. Samarasinghe. “Modelling the dynamics of CaMKIINMDAR complex related to memory formation in synapses: The possible roles of threonine 286 autophosphorylation of CaMKII in long term potentiation”. In: *Journal of Theoretical Biology* 365 (2015), pp. 403–419. ISSN: 0022-5193. DOI: <https://doi.org/10.1016/j.jtbi.2014.11.001>. URL: <http://www.sciencedirect.com/science/article/pii/S002251931400633X>.
- [Lis17] John Lisman. “Criteria for identifying the molecular basis of the engram (CaMKII, PKMzeta)”. In: *Molecular Brain* 10 (Nov. 2017), pp. 55–. ISSN: 1756-6606. URL: <http://www.ncbi.nlm.nih.gov/pmc/articles/PMC5707903/>.
- [Lis85] J E Lisman. “A mechanism for memory storage insensitive to molecular turnover: a bistable autophosphorylating kinase.” In: *Proceedings of the National Academy of Sciences of the United States of America* 82.9 (May 1985), pp. 3055–3057. ISSN: 1091-6490. URL: <http://www.ncbi.nlm.nih.gov/pmc/articles/PMC397705/>.

- [Lis89] J Lisman. “A mechanism for the Hebb and the anti-Hebb processes underlying learning and memory.” In: *Proceedings of the National Academy of Sciences of the United States of America* 86.23 (Dec. 1989), pp. 9574–9578. ISSN: 1091-6490. URL: <http://www.ncbi.nlm.nih.gov/pmc/articles/PMC298540/>.
- [LSC02] John Lisman, Howard Schulman, and Hollis Cline. “The molecular basis of CaMKII function in synaptic and behavioural memory”. In: *Nature Reviews Neuroscience* 3 (Mar. 2002), pp. 175–. URL: <http://dx.doi.org/10.1038/nrn753>.
- [LSL12] Lu Li, Melanie I. Stefan, and Nicolas Le Novère. “Calcium Input Frequency, Duration and Amplitude Differentially Modulate the Relative Activation of Calcineurin and CaMKII”. In: *PLOS ONE* 7.9 (Sept. 2012), pp. 1–17. DOI: [10.1371/journal.pone.0043810](https://doi.org/10.1371/journal.pone.0043810). URL: <https://doi.org/10.1371/journal.pone.0043810>.
- [LYR12] John Lisman, Ryohei Yasuda, and Sridhar Raghavachari. “Mechanisms of CaMKII action in long-term potentiation”. In: *Nat Rev Neurosci* 13.3 (Mar. 2012). 22334212[pmid], pp. 169–182. ISSN: 1471-003X. DOI: [10.1038/nrn3192](https://doi.org/10.1038/nrn3192). URL: <http://www.ncbi.nlm.nih.gov/pmc/articles/PMC4050655/>.
- [Mal+88] RC Malenka et al. “Postsynaptic calcium is sufficient for potentiation of hippocampal synaptic transmission”. In: *Science* 242.4875 (1988), pp. 81–84. ISSN: 0036-8075. DOI: [10.1126/science.2845577](https://doi.org/10.1126/science.2845577). eprint: <http://science.scienmag.org/content/242/4875/81.full.pdf>. URL: <http://science.scienmag.org/content/242/4875/81>.
- [MGS12] Henry Markram, Wulfram Gerstner, and Per Jesper Sjöström. “Spike-Timing-Dependent Plasticity: A Comprehensive Overview”. In: *Frontiers in Synaptic Neuroscience* 4 (2012), p. 2. ISSN: 1663-3563. DOI: [10.3389/fnsyn.2012.00002](https://doi.org/10.3389/fnsyn.2012.00002). URL: <https://www.frontiersin.org/article/10.3389/fnsyn.2012.00002>.
- [Mic13] PJ Michalski. “The Delicate Bistability of CaMKII”. In: *Biophysical Journal* 105.3 (June 2013), pp. 794–806. ISSN: 1542-0086. URL: <http://www.ncbi.nlm.nih.gov/pmc/articles/PMC3736660/>.
- [Moz+17] P. Mozgunov et al. “A review of the deterministic and diffusion approximations for stochastic chemical reaction networks”. In: *ArXiv e-prints* (Nov. 2017). arXiv: [1711.02567 \[math.PR\]](https://arxiv.org/abs/1711.02567).
- [NC17] Wilten Nicola and Claudia Clopath. “Supervised learning in spiking neural networks with FORCE training”. In: *Nature Communications* 8.1 (2017), p. 2208. ISSN: 2041-1723. DOI: [10.1038/s41467-017-01827-3](https://doi.org/10.1038/s41467-017-01827-3). URL: <https://doi.org/10.1038/s41467-017-01827-3>.
- [OLD15] Gabriel Koch Ocker, Ashok Litwin-Kumar, and Brent Doiron. “Self-Organization of Microcircuits in Networks of Spiking Neurons with Plastic Synapses”. In: *PLOS Computational Biology* 11.8 (Aug. 2015), pp. 1–40. DOI: [10.1371/journal.pcbi.1004458](https://doi.org/10.1371/journal.pcbi.1004458). URL: <https://doi.org/10.1371/journal.pcbi.1004458>.
- [Opa+10] Patricio Opazo et al. “CaMKII Triggers the Diffusional Trapping of Surface AMPARs through Phosphorylation of Stargazin”. In: *Neuron* 67.2 (2010), pp. 239–252. ISSN: 0896-6273. DOI: <https://doi.org/10.1016/j.neuron.2010.06.007>. URL: <http://www.sciencedirect.com/science/article/pii/S0896627310004654>.
- [OWW05] Daniel H. O’Connor, Gayle M. Wittenberg, and Samuel S.-H. Wang. “Dissection of Bidirectional Synaptic Plasticity Into Saturable Unidirectional Processes”. In: *Journal of Neurophysiology* 94.2 (Aug. 2005), pp. 1565–1573. ISSN: 0022-3077. DOI: [10.1152/jn.00047.2005](https://doi.org/10.1152/jn.00047.2005). URL: <https://doi.org/10.1152/jn.00047.2005>.
- [Pep+10] Shirley Pepke et al. “A Dynamic Model of Interactions of Ca(2+), Calmodulin, and Catalytic Subunits of Ca(2+)/Calmodulin-Dependent Protein Kinase II”. In: *PLoS Computational Biology* 6.2 (Jan. 2010), e1000675–. ISSN: 1553-7358. URL: <http://www.ncbi.nlm.nih.gov/pmc/articles/PMC2820514/>.
- [PG06] Jean-Pascal Pfister and Wulfram Gerstner. “Triplets of Spikes in a Model of Spike Timing-Dependent Plasticity”. In: *Journal of Neuroscience* 26.38 (2006), pp. 9673–9682. ISSN: 0270-6474. DOI: [10.1523/JNEUROSCI.1425-06.2006](https://doi.org/10.1523/JNEUROSCI.1425-06.2006). eprint: <http://www.jneurosci.org/content/26/38/9673.full.pdf>. URL: <http://www.jneurosci.org/content/26/38/9673>.

- [Ros+17] Tom Rossetti et al. “Memory Erasure Experiments Indicate a Critical Role of CaMKII in Memory Storage”. In: *Neuron* 96.1 (Sept. 2017), 207–216.e2. ISSN: 0896-6273. DOI: [10.1016/j.neuron.2017.09.010](https://doi.org/10.1016/j.neuron.2017.09.010). URL: <https://doi.org/10.1016/j.neuron.2017.09.010>.
- [SA09] David Sussillo and L. F. Abbott. “Generating Coherent Patterns of Activity from Chaotic Neural Networks”. In: *Neuron* 63.4 (Aug. 2009). 19709635[pmid], pp. 544–557. ISSN: 0896-6273. DOI: [10.1016/j.neuron.2009.07.018](https://doi.org/10.1016/j.neuron.2009.07.018). URL: <http://www.ncbi.nlm.nih.gov/pmc/articles/PMC2756108/>.
- [SBC02] Harel Z. Shouval, Mark F. Bear, and Leon N Cooper. “A unified model of NMDA receptor-dependent bidirectional synaptic plasticity”. In: *Proceedings of the National Academy of Sciences* 99.16 (2002), pp. 10831–10836. ISSN: 0027-8424. DOI: [10.1073/pnas.152343099](https://doi.org/10.1073/pnas.152343099). eprint: <http://www.pnas.org/content/99/16/10831.full.pdf>. URL: <http://www.pnas.org/content/99/16/10831>.
- [Shi+06] Julia M Shifman et al. “Ca(2+)/calmodulin-dependent protein kinase II (CaMKII) is activated by calmodulin with two bound calciums”. In: *Proceedings of the National Academy of Sciences of the United States of America* 103.38 (Sept. 2006), pp. 13968–13973. ISSN: 1091-6490. URL: <http://www.ncbi.nlm.nih.gov/pmc/articles/PMC1599897/>.
- [SL13] Magdalena Sanhueza and John Lisman. “The CaMKII/NMDAR complex as a molecular memory”. In: *Molecular Brain* 6 (Jan. 2013), pp. 10–10. ISSN: 1756-6606. URL: <http://www.ncbi.nlm.nih.gov/pmc/articles/PMC3582596/>.
- [Son00] Abbott L. F. Song Sen Miller Kenneth D. “Competitive Hebbian learning through spike-timing-dependent synaptic plasticity”. In: *Nature Neuroscience* 3.2000/09/01/online (2000). <http://dx.doi.org/10.1038/78829>, p. 919.
- [Str00] Steven H. Strogatz. *Nonlinear Dynamics and Chaos: With Applications to Physics, Biology, Chemistry and Engineering*. Westview Press, 2000.
- [Tom+05] Susumu Tomita et al. “Bidirectional Synaptic Plasticity Regulated by Phosphorylation of Stargazin-like TARPss”. In: *Neuron* 45.2 (Jan. 2005), pp. 269–277. ISSN: 0896-6273. DOI: [10.1016/j.neuron.2005.01.009](https://doi.org/10.1016/j.neuron.2005.01.009). URL: <https://doi.org/10.1016/j.neuron.2005.01.009>.
- [Ura+08] Hideyoshi Urakubo et al. “Requirement of an Allosteric Kinetics of NMDA Receptors for Spike Timing-Dependent Plasticity”. In: *Journal of Neuroscience* 28.13 (2008), pp. 3310–3323. ISSN: 0270-6474. DOI: [10.1523/JNEUROSCI.0303-08.2008](https://doi.org/10.1523/JNEUROSCI.0303-08.2008). eprint: <http://www.jneurosci.org/content/28/13/3310.full.pdf>. URL: <http://www.jneurosci.org/content/28/13/3310>.
- [VVT18] Gaëtan Vignoud, Laurent Venance, and Jonathan D. Touboul. “Interplay of multiple pathways and activity-dependent rules in STDP”. In: *PLOS Computational Biology* 14.8 (Aug. 2018), pp. 1–32. DOI: [10.1371/journal.pcbi.1006184](https://doi.org/10.1371/journal.pcbi.1006184). URL: <https://doi.org/10.1371/journal.pcbi.1006184>.
- [Wan+05] John Q. Wang et al. “Phosphorylation of AMPA receptors”. In: *Molecular Neurobiology* 32.3 (Dec. 2005), pp. 237–249. ISSN: 1559-1182. DOI: [10.1385/MN:32:3:237](https://doi.org/10.1385/MN:32:3:237). URL: <https://doi.org/10.1385/MN:32:3:237>.
- [Zha00] A. M. Zhabotinsky. “Bistability in the Ca(2+)/calmodulin-dependent protein kinase-phosphatase system.” In: *Biophys J* 79.5 (Nov. 2000). 11053103[pmid], pp. 2211–2221. ISSN: 0006-3495. URL: <http://www.ncbi.nlm.nih.gov/pmc/articles/PMC1301111/>.

Appendices

Appendix A

Supplementary figures and tables

Parameters	Unit	Definition	Figs 3.6 & 3.8	Fig4.4
C_{pre}		Amplitude of presynaptic calcium bump	0.4	0.4
C_{post}		Amplitude of postsynaptic calcium bump	0.84	0.84
θ_{pot}	μM	Calcium threshold for potentiation	1.08	1.08
γ_{pot}	μM	Intensity of potentiation above threshold	120	380
θ_{dep}	μM	Calcium threshold for depression	1	1.05
γ_{dep}	μM	Intensity of depression above threshold	200	200
r_{damp}		Saturation factor	0.3	0.3
τ_{Ca}	ms	Time constant for calcium	80	30
τ_ρ	s	Time constant for phosphorylation level	100	250
τ_w	s	Time constant for synaptic weight	200	250
τ_x	ms	Time constant for recuperation variables	100	100
D	ms	Transmission delay from pre to post	15	5
ρ_{max}	μM	Max concentration of active CaMKII subunits	200	200
ρ_{crit}	μM	Limit of basins of attraction at basal calcium level	40	100
σ	$(\mu M)^{\frac{1}{2}}$	Base level of noise (when assumed independent of t_{bas})	25	25

Table A.1: Value of synapse parameters used for the simulations presented in this report

N	N_E	N_I	ϵ	g	$\frac{\nu_{ext}}{\nu_{thr}}$
400	320	80	0.1	2	3

Table A.2: Value of network parameters used for simulation shown in Fig4.4

Appendix B

Equations for the fine-grain model in the general case

B.1 Equations for the detailed model

Here I focus on the fine-grain model that we have studied. This model is a generalization of Graupner and Brunel 2007 when the concentration of available calcium-bound calmodulin is allowed to fluctuate, and where CaMKII subunits can be phosphorylated at the T305/306 site. I will derive the equations of the model and then focus on the difficulties that we face to simulate the general case.

In all that follows, $[Ca^{2+}]$ represents the concentration of Ca^{2+} ions in the postsynaptic spine.

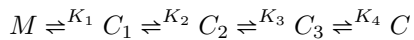
B.1.1 Calmodulin binding to calcium

Calmodulin can bind to calcium at four sites. The protein has two lobes (N and C lobes). Each lobe can bind to two Ca^{2+} ions in a highly cooperative manner. The two binding sites of a same lobe are often considered as interchangeable, and we therefore refer to possible states of calmodulin as $Apo - CaM$ (no calcium ion bound on either lobe), and states $(N_i C_j - CaM)_{(i,j) \in \{1,2\}^2}$, where i and j denote the number of Ca^{2+} ions bound at each lobe of the protein.

It is often considered that $N_2 C_2 - CaM$ has much greater affinity to CaMKII subunits than other forms of non-complete calmodulin. Therefore, many models of CaMKII activation assume that only fully-bound calmodulin ($N_2 C_2 - CaM$) can bind to CaMKII subunits.

In Pepke et al. 2010, a model of interaction between calcium ions and calmodulin is derived. The authors conclude that partially-calcium-bound calmodulin forms can also bind to CaMKII (see in particular Fig7 of their paper), and that this interaction is especially important for the onset of activation of CaMKII. In our model we do assume that only $N_2 C_2 - CaM$ bind to CaMKII for simplicity, and we forego modeling of the lobes of calmodulin, focusing only on the amount of calcium ions that are bound to it. This is an approximation as cooperativity in binding is dependent on the spatial configuration of calmodulin.

We assume a total concentration of calmodulin CaM_0 , and introduce states and transitions:



Here M is the concentration of $Apo - CaM$, and C is the concentration of fully-bound $Ca^{2+} - CaM$.

We will assume that calcium binding to calmodulin is much faster than the characteristic time of variation of $[Ca^{2+}]$. This yields:

$$\begin{aligned}
\frac{dC_1}{dt} &= k_1 M [Ca_{2+}] - k_2 C_1 - k_{-1} C_1 + k_{-2} C_2 &= 0 \\
\frac{dC_2}{dt} &= k_2 C_1 [Ca_{2+}] - k_3 C_2 - k_{-2} C_2 + k_{-3} C_3 &= 0 \\
\frac{dC_3}{dt} &= k_3 C_2 [Ca_{2+}] - k_4 C_3 - k_{-3} C_3 + k_{-4} C &= 0 \\
\frac{dC}{dt} &= k_4 C_3 [Ca_{2+}] - k_{-4} C &= 0
\end{aligned}$$

$CaM_0 = M + C_1 + C_2 + C_3 + C$

The last equation is the law of conservation of total calmodulin. One can derive the concentration of fully-bound calmodulin as a function of $[Ca^{2+}]$:

$$C = \frac{CaM_0}{1 + \frac{K_4}{[Ca^{2+}]} + \frac{K_3 K_4}{[Ca^{2+}]^2} + \frac{K_2 K_3 K_4}{[Ca^{2+}]^3} + \frac{K_1 K_2 K_3 K_4}{[Ca^{2+}]^4}}$$

In the following we use notation C to refer either to a fully-bound calmodulin or to its concentration in the postsynaptic spine, depending on context.

B.1.2 Calmodulin binding and phosphatase kinetics

Figure B.1 defines the reaction constants for all reactions involving CaMKII subunits.

In the general model, a CaMKII subunit can be in one of six states, as defined by FigB.2. The first index of a state indicates phosphorylation of Threonine-286 of the subunit, while the second index indicates phosphorylation at the Threonine-305/306 site, considered as a single site for phosphorylation. For instance, a CaMKII subunit in the state D_{up} would be unphosphorylated at T-286 and phosphorylated at the T-305/306 site. Because it is not possible to be both phosphorylated at site T-305/306 and bound to calmodulin (binding of calmodulin physically blocks the access to the T-305/306 phosphorylation site), we denote C_u the state for CaMKII that is unphosphorylated at T-286 and bound to calmodulin.

Let us define γ as the fraction of CaMKII subunits not phosphorylated at site T-286 that are bound to a C . We also define quantities γ^* as the fraction of CaMKII subunits phosphorylated at site T-286 that are bound to a C , ζ as the fraction of CaMKII subunits unphosphorylated at site T-305/306 that are bound to a C , and ζ^* as the fraction of CaMKII subunits phosphorylated at site T-305/306 that are bound to a C :

$$\begin{aligned}
\gamma &= \frac{C_u}{D_{up} + D_{uu} + C_u} \\
\gamma^* &= \frac{C_p}{D_{pp} + D_{pu} + C_p} \\
\zeta &= \frac{D_{up}}{D_{up} + D_{uu} + C_u} \\
\zeta^* &= \frac{C_u}{D_{pp} + D_{pu} + C_p}
\end{aligned}$$

In what follows, we assume that binding of different calmodulin proteins to the subunits of a same ring CaMKII are independent events. With this assumption, C only influences the evolution of CaMKII through γ , γ^* , ζ and ζ^* .

To find those four quantities, one must make assumptions as to the kinetics of the model. Here we assume that calmodulin binding and T-305/306 phosphorylation are always at equilibria with the concentration of available C , of available CaMKII subunits and of active phosphatase $PP1_{act}$ (ie those are infinitely fast relatively to the speed of variation of available species).

The equilibrium of calmodulin binding, respectively to T286-unphosphorylated and T286-phosphorylated species provides:

$$[(1 - \gamma - \zeta)(C - \gamma S_u - \gamma^* S_p) - K_5 \gamma] S_u = 0 \quad (\text{B.1})$$

$$[(1 - \gamma^* - \zeta^*)(C - \gamma S_u - \gamma^* S_p) - K_9 \gamma^*] S_p = 0 \quad (\text{B.2})$$

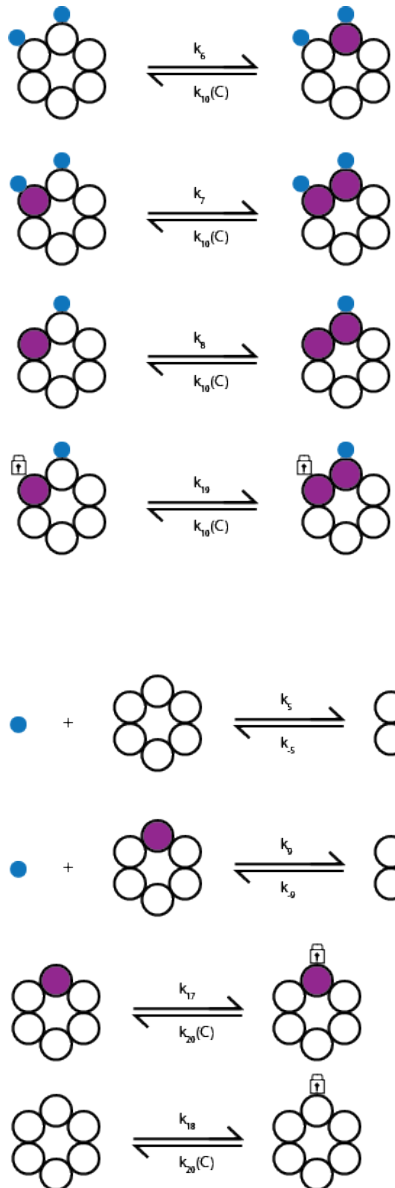


Figure B.1: Definition of the different reaction constants involving CaMKII. Blue circles indicate calcium-calmodulin. In the models studied here we assume that only fully-loaded (four Ca^{2+}) calmodulin molecules can interact with other messengers, including CaMKII. Phosphorylated sub-units are filled in purple

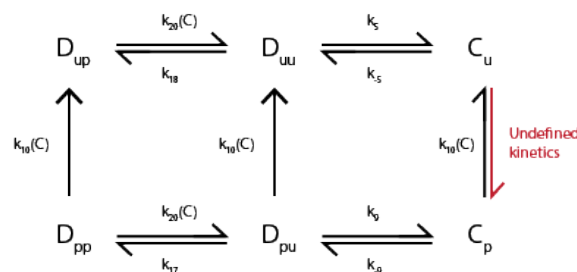


Figure B.2: Graph of the different CaMKII sub-unit states and their transitions in the model of Michalski 2014. Michalski chose to take into account phosphorylation at the Threonine-305/306 sites, as it changes the qualitative behavior of phosphorylation at the synapse. In this setting, each sub-unit can be in one of six states.

The equilibrium of the T-305 phosphorylation/dephosphorylation reaction provides:

$$[k_{18}(1 - \gamma - \zeta - k_{10}(C)\gamma[PP1]_{act}]S_u = 0 \quad (\text{B.3})$$

$$[k_{17}(1 - \gamma^* - \zeta^* - k_{10}(C)\gamma^*[PP1]_{act}]S_p = 0 \quad (\text{B.4})$$

In [B.1](#) S_p is the total concentration of phosphorylated subunits, $S_u = 6 * CaMKII_0 - S_p$ the total concentration of unphosphorylated subunits. Those quantities are formally introduced in the next subsection. They reflect the concentration of the different states of CaMKII complexes and the number of phosphorylated subunits of each of these states.

Other terms seen in [B.1](#) to [B.4](#) are reaction constants K_5 and K_9 (see [B.1](#) for definitions) and $k_{10}(C)$, which is the reaction constant for phosphatase (ie de-phosphorylation) of CaMKII subunits by activated protein phosphatase 1 (PP1). $k_{10}(C)$ can be expressed from parameters $k_{11}, k_{-11}, k_{12}, k_{13}, k_{-13} \dots$.

Consider the linear system resulting from the equilibria of the binding of active $PP1$ to CaMKII subunits:

$$(k_{12} + k_{-11})[D_{pu}PP1] = k_{11}[D_{pu}][PP1_{free}] \quad (\text{B.5})$$

$$(k_{12} + k_{-11})[C_pPP1] = k_{11}[C_p][PP1_{free}] \quad (\text{B.6})$$

$$(k_{12} + k_{-11})[D_{pp}PP1_{286}] = k_{11}[D_{pp}][PP1_{free}] \quad (\text{B.7})$$

$$(k_{14} + k_{-13})[D_{pp}PP1_{305}] = k_{13}[D_{pp}][PP1_{free}] \quad (\text{B.8})$$

$$(k_{16} + k_{-15})[D_{up}PP1] = k_{15}[D_{up}][PP1_{free}] \quad (\text{B.9})$$

$$0 = [D_{pu}PP1] + [C_pPP1] + [D_{pp}PP1_{286}] + [D_{pp}PP1_{305}] + [D_{up}PP1] + [PP1_{free}] \quad (\text{B.10})$$

The last equation in [B.10](#) is the conservation of total active $PP1$. Solving this linear system provides k_{10} :

$$k_{10} = \frac{k_{12}}{\frac{k_{12} + k_{-11}}{k_{11}} + [D_{pu}] + [C_p] + (1 + \frac{(k_{12} + k_{-11})k_{13}}{(k_{14} + k_{-13})k_{11}})[D_{pp}] + \frac{(k_{12} + k_{-11})k_{15}}{(k_{16} + k_{-15})k_{11}}[D_{up}]} \quad (\text{B.11})$$

This expression can be simplified when one can assume that the action of phosphatase at the different sites of a CaMKII subunit occur at the same rates. Then defining $K_M = \frac{k_{12} + k_{-11}}{k_{11}}$, one obtains:

$$k_{10} = \frac{k_{12}}{K_M + (1 + \zeta^*)S_p + \zeta S_u} \quad (\text{B.12})$$

Here one must keep in mind the pathway (see [Fig2.5](#)) that stems from variations in $[Ca^{2+}]$ and results in variations in the concentration of CaMKII in the different states. Here ζ, ζ^*, S_u, S_p all vary with time, and so does k_{10} .

B.1.3 CaMKII states

Here we consider CaMKII rings with six subunits, each bound to the rest by their hub region. Each subunit of the holoenzyme can phosphorylate its neighbor at T-286 site only in a given direction, which is the same for all subunits. One can use symmetry arguments to reduce the number of possible states for a CaMKII ring. [Fig2.8](#) defines those states. In this figure, each red arrow represents a transition from one state to another by phosphorylation k_6 , each green arrow represents a transition by phosphorylation k_7 or k_8 . Phosphate are not represented, but are all assumed to occur at (variable) speed k_{10} .

Based on this transition diagram, and assuming that both calmodulin binding events and T-305-306 phosphorylation events occur independently from other similar events, one obtains the following system of equations:

$$\begin{aligned}
dS_0 &= \left(-6k_6\gamma^2 S_0 + \eta S_1 \right) dt \\
dS_1 &= \left(6k_6\gamma^2 S_0 - 4k_6\gamma^2 S_1 - \gamma\xi S_1 + 2\eta(S_2 + S_3 + S_4) - \eta S_1 \right) dt \\
dS_2 &= \left(k_6\gamma^2 S_1 - 3k_6\gamma^2 S_2 + \gamma\xi S_1 - \gamma\xi S_2 + 3\eta(S_5 + S_6 + S_7 + S_8) - 2\eta S_2 \right) dt \\
dS_3 &= \left(2k_6\gamma^2 S_1 - 3k_6\gamma^2 S_3 - \gamma\xi S_3 + 3\eta(S_5 + S_6 + S_7 + S_8) - 2\eta S_3 \right) dt \\
dS_4 &= \left(k_6\gamma^2 S_1 - 2k_6\gamma^2 S_4 - 2\gamma\xi S_4 + 3\eta(S_5 + S_6 + S_7 + S_8) - 2\eta S_4 \right) dt \\
dS_5 &= \left(k_6\gamma^2(S_2 + S_3) - 2k_6\gamma^2 S_5 + \gamma\xi S_2 - \gamma\xi S_5 + 4\eta(S_9 + S_{10} + S_{11}) - 3\eta S_5 \right) dt \\
dS_6 &= \left(k_6\gamma^2(S_2 + S_3) - k_6\gamma^2 S_6 + 2\gamma\xi S_4 - 2\gamma\xi S_6 + 4\eta(S_9 + S_{10} + S_{11}) - 3\eta S_6 \right) dt \\
dS_7 &= \left(k_6\gamma^2(S_2 + 2S_4) - k_6\gamma^2 S_7 + \gamma\xi S_3 - 2\gamma\xi S_7 + 4\eta(S_9 + S_{10} + S_{11}) - 3\eta S_7 \right) dt \\
dS_8 &= \left(k_6\gamma^2 S_3 - 3\gamma\xi S_8 + 4\eta(S_9 + S_{10} + S_{11}) - 3\eta S_8 \right) dt \\
dS_9 &= \left(k_6\gamma^2 S_5 - k_6\gamma^2 S_9 + \gamma\xi(S_6 + S_7) - \gamma\xi S_9 + 5\eta S_{12} - 4\eta S_9 \right) dt \\
dS_{10} &= \left(k_6\gamma^2(S_5 + S_6) + \gamma\xi(S_7 + S_8) - 2\gamma\xi S_{10} + 5\eta S_{12} - 4\eta S_{10} \right) dt \\
dS_{11} &= \left(k_6\gamma^2 S_7 + \gamma\xi S_6 - 2\gamma\xi S_{11} + 5\eta S_{12} - 4\eta S_{11} \right) dt \\
dS_{12} &= \left(k_6\gamma^2 S_9 + \gamma\xi(S_9 + 2S_{10} + 2S_{11}) - \gamma\xi S_{12} + 6\eta S_{13} - 5\eta S_{12} \right) dt \\
dS_{13} &= \left(\gamma\xi S_{12} - 6\eta S_{13} \right) dt
\end{aligned} \tag{B.13}$$

In these equations we have defined $\eta = k_{10}(1 + \eta^*)$ and $\xi = k_7\gamma^* + k_8(1 - \gamma^* - \eta^*) + k_{19}\zeta^*$

State 4 has $m_4 = 2$ phosphorylated subunits, state 8 has $m_8 = 3$. In general, denoting m_i the number of phosphorylated subunits of state i of the CaMKII complex, we can define the total concentration of phosphorylated subunits as:

$$S_p = \sum_{i=0}^{13} m_i S_i \tag{B.14}$$

Also define $S_u = 6 * [CaMKII]_0 - S_p$ to have all quantities in our equations defined.

B.2 On solving the general CaMKII system

Here one must notice that equations ?? depend on the concentrations at the subunit level ($[D_{uu}], [C_u], \dots$) through fractions γ , γ^* , ζ and ζ^* . However, those four quantities are determined by equations B.1 to B.4, which depend on the phosphatase rate k_{10} . As equation B.12 indicates, this reaction rate itself depends on S_p and S_u , which are variables defined from the ring-level states $(S_i)_{i \in 1..13}$.

This makes the system hard to integrate directly. The way we proceeded to simulate its evolution was to alternate between a step of solving B.1 to B.12, and a step of integration of ???. However, it seems that we ran into a singularity that precludes us from going very far into the simulation from many initial conditions. It may be required for someone with more expertise on numerical stability to investigate the system so that we can move forward on the general case.

It seems easier to simulate the system when phosphorylation at the T-305/306 site is not taken into account. This corresponds to the previous equations when $\zeta = \zeta^* = 0$. Fig2.11 is an example of our results on this case, starting from a low concentration of phosphorylated subunits S_p .

Appendix C

Tentative models of action of CaMKII on synaptic strength

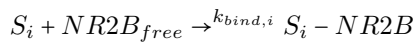
C.1 CaMKII binding to NMDA receptors

If the induction of LTP requires activable (T-286) CaMKII in the postsynaptic spine, several studies (Gardoni, Caputi, and Cimino 1998, John Lisman, Yasuda, and Raghavachari 2012) have shown that the binding of CaMKII to the NR2B subunit of NMDA receptors at the postsynaptic membrane is necessary for retention. In other words, the bistable switch in J. E. Lisman 1985 would not be the concentration of active CaMKII in the cytosol, but the concentration of CaMKII-NR2B complexes at the membrane. Sanhueza and John Lisman 2013 suggests that the CaMKII-NR2B complexes could embody a molecular tag that would trigger the structural and epigenetic processes of late LTP. When bound to NR2B at the membrane, CaMKII subunits are harder to dephosphorylate, and binding to calmodulin is enhanced. Moreover, phosphorylated subunits can phosphoryate the AMPA receptors within their reach: a CaMKII holoenzyme can be bound to a NMDA receptor at up to two spots, and can also be tied to the membrane via scaffold proteins, actin and densin (see Hell 2014).

We followed experimental results in Bayer et al. 2001 to develop a model of CaMKII binding to NMDA and phosphorylating AMPA receptors at the membrane.

Note that only some CaMKII can bind to NMDA (α -CaMKII). Binding can occur onto the subunit 2B of a NMDA receptor (or NR2B). It required the binding CaMKII subunit to either be phosphorylated at T-286 or carry a $Ca^{2+} - CaM$. Calmodulin dissociates from unphosphorylated kinase that is not complexed with NR2B with an off-rate of approx $2s^{-1}$. Finally, binding to NR2B precludes phosphorylation of the bound subunit at T305/306.

Assume a population of M NMDA receptors at the PSD. Here we will assume a single binding site per NMDA receptor. Denote $k_{bind,i} = m_i k_{bind}$ as defined by:



Consider $\mu_i = [S_i - NB2B]$ and $\mu = \sum_{i=0}^{13} \mu_i$. Finally, define $U = \sum_{i=0}^{13} (m_i - 1)\mu_i$ which represents the concentration of subunits at the membrane available to phosphorylate AMPAs in the case that a CaMKII holoenzyme only uses one of its phosphorylated subunits to bind to a NR2B.

In that case, the variable of interest to study phosphorylation would be the number of CaMKII-NR2B complexes (or equivalently, μ). one can then investigate if this quantity is bistable under a principle similar to J. E. Lisman 1985. Qualitatively, the interactions are close to the same. Diagram 2.5 is still valid if we change K_1 from CaMKII to CaMKII-NR2B. Quantitatively, interaction with NR2B changes affinities with both CaM and PP1, modifying the speed of kinase and phosphatase. These changes go in the direction of greater stability of the high activation state (CaM trapping by CaMKII, CaMKII trapping by NR2B).

C.2 Phosphorylation of AMPA receptors

Given the previous definitions, one can write:

$$\begin{cases} \frac{dU}{dt} = k_{bind}(M - \mu) \sum_{i=0}^{13} m_i(m_i - 1)S_i - \sum_{i=0}^{13} (m_i - 1)k_{unbind}[PP1_{membrane}] \\ \frac{d\mu}{dt} = k_{bind}(M - \mu) \sum_{i=0}^{13} (m_i S_i) - 14k_{unbind}[PP1_{membrane}] \end{cases} \quad (\text{C.1})$$

In turn, AMPA phosphorylation is controlled by the CaMKII that are part of a ring that is bound to NR2B at the membrane, who are phosphorylated at T-286 but are not themselves bound to NR2B. The speed of phosphorylation thus contains a term proportionnal to U .

Here we will assume that AMPA receptors can be in four states of conductance, according to experimental data. Denote n the total number of AMPA receptors at the PSD, and n_j the number of receptors in conductance state j , with conductance g_j .

A first linear model of phosphorylation would be:

$$\frac{dn_0}{dt} = -r_{phos,0}n_0U + r_{pase,0}n_1[PP1_{membrane}] \quad (\text{C.2})$$

$$\frac{dn_1}{dt} = r_{phos,1}(n_0 - n_1)U + r_{pase,1}(n_2 - n_1)[PP1_{membrane}] \quad (\text{C.3})$$

$$\frac{dn_2}{dt} = r_{phos,2}(n_1 - n_2)U + r_{pase,2}(n_3 - n_2)[PP1_{membrane}] \quad (\text{C.4})$$

$$\frac{dn_3}{dt} = r_{phos,3}(n_2 - n_3)U - r_{pase,3}n_3[PP1_{membrane}] \quad (\text{C.5})$$

$$(\text{C.6})$$

Let us for now ignore the role of AMPA receptor diffusion and the fact that the flux of neurotransmitters is higher at the center of the PSD than in the periphery. We can consider that all AMPA receptors have the same expectation in number of neurotransmitters received in response to a presynaptic stimulus. Without any spatial dimension to the problem, the postsynaptic component of the synaptic weight depends on the number of AMPA receptors in each conductance state:

$$w = \sum_{j=0}^3 g_j n_j$$

Note that w would reflect a long term synaptic weight. Short-term effects like transient deactivation of AMPA receptors is not taken into account here.

C.3 Quantification noise in the system

C.3.1 Noise on cytosolic variables

If we take into account the finite number number of CaMKII molecule in the cytosol, what would the noise look like on the phosphorylation variable S_p ?

We used Langevin approximation on the different states of CaMKII holoenzymes to describe the influence of quantification noise in our fine-grain model (see Mozgunov et al. 2017). To each transition in Fig2.8 we associate a process $W_{i,j}$.

The equations B.13 would be modified like so:

$$\begin{aligned}
dS_0 &= \left(-6k_6\gamma^2 S_0 + \eta S_1 \right) dt \\
&\quad + \frac{1}{\sqrt{N_A V}} \left(-\sqrt{6k_6\gamma^2 S_0 + \eta S_1} dW_{0,1} \right) \\
dS_1 &= \left(6k_6\gamma^2 S_0 - 4k_6\gamma^2 S_1 - \gamma\xi S_1 + 2\eta(S_2 + S_3 + S_4) - \eta S_1 \right) dt \\
&\quad + \frac{1}{\sqrt{N_A V}} \left(\sqrt{6k_6\gamma^2 S_0 + \eta S_1} dW_{0,1} \right. \\
&\quad - \sqrt{k_6\gamma^2 S_1 + \gamma\xi S_1 + 2\eta S_2} dW_{1,2} \\
&\quad - \sqrt{2k_6\gamma^2 S_1 + 2\eta S_3} dW_{1,3} \\
&\quad \left. - \sqrt{2k_6\gamma^2 S_1 + 2\eta S_4} dW_{1,4} \right) \\
dS_2 &= \left(k_6\gamma^2 S_1 - 3k_6\gamma^2 S_2 + \gamma\xi S_1 - \gamma\xi S_2 + 3\eta(S_5 + S_6 + S_7 + S_8) - 2\eta S_2 \right) dt \\
&\quad + \frac{1}{\sqrt{N_A V}} \left(\sqrt{k_6\gamma^2 S_1 + \gamma\xi S_1 + 2\eta S_2} dW_{1,2} \right. \\
&\quad - \sqrt{k_6\gamma^2 S_2 + \gamma\xi S_2 + 3\eta S_5} dW_{2,5} \\
&\quad \left. - \sqrt{\dots} dW_{2,6} - \sqrt{\dots} dW_{2,7} - \sqrt{\dots} dW_{2,8} \right) \\
&\dots = \dots
\end{aligned}$$

Here all $W_{i,j}$ are considered to be independent. The noise W_p on S_p ends up being a Gaussian process with infinitesimal variance the sum of all positive terms in B.13. Knowing the nature of this noise is helpful for analyzing a set of trajectories in Fig3.4. This means that **under quantification noise** as well as any other source of noise such that W_p remains Gaussian, we have an analytical formula for finding $w = f(\rho_{bas}, t_{bas})$, the final average synaptic strength at $A \Rightarrow B$ as a function of the activation state when calcium goes back to basal level and the time spent above basal level.

C.3.2 Noise at the membrane

As stressed in Hell 2014, there are only between 10 and 30 NMDA receptors at the PSD. It is expected that between 50 and 200 CaMKII molecules could be in proximity of those receptors at the membrane. Even though a CaMKII can bind at a membrane not only with NR2B, but also with actin, densin and scaffold molecules, one can expect a bit more CaMKII bound than there are available NR2B. However, That would still mean that only a few molecules would implement the tag mentionned in Sanhueza and John Lisman 2013.

The nature of the process μ when considering quantification noise in our model of CaMKII-NR2B interaction remains to be found. The problem can be framed as: *What is μ , where*

$$d\mu = c_1 S_p dt - c_2 dt$$

with

$$dS_p = \sum_{i=0}^{13} m_i dS_i$$